October 15, 2018

DESIGN AND OPTIMIZATION OF W-TAILORED OPTICAL FIBER

Kyevuga Simon Peter

MSEE 1163-03216-08406

A Thesis Submitted to the Department of Electrical, Telecommunication and Computer Engineering, School of Engineering and Applied Sciences, Kampala International University, Uganda, in Partial Fulfillment for the Award of the Degree of Master of Science in Electrical Engineering (MSEE)

OCTOBER, 2018

DECLARATION

I Kyevuga Simon Peter, do hereby declare that this thesis entitled: "**Design and Optimization of W-Tailored Optical Fiber**" has never been submitted as a requirement for the award of any degree in any academic institution world wide. All citations are duly acknowledged by means of reference.

Signature and Date..

Kyevuga Simon Peter

MSEE: 1163-03216-08406

CERTIFICATION

This is to certify that the thesis entitled "**Design and Optimization of W-Tailored Optical Fiber** " by Kyevuga Simon Peter: MSEE: 1163-03216-08406 was carried out under our supervision.

Signature and Date..

Dr. Sani Sulaiman

Supervisor I

Signature and Date..

Ms. Zaina Kalyankolo

Supervisor II

ACKNOWLEDGEMENT

I am indebted to my Main Supervisor Dr. Sani Sulaiman for his support, guidance, encouragement and contribution towards the success of this project. I would like to acknowledge the assistance of my Co-supervisor; Ms. Zaina Kalyankore during the project. I equally extend my gratitude to all my relatives and family member for their financial support. God bless you all abundantly.

DEDICATION

I dedicate this research work to my parents, relatives and friends for their support towards my Education. I also convey my heartfelt gratitude to the almighty Lord who has granted me his grace in whatever things I am doing.

Contents

List of Tables

List of Figures

List of Abbreviations

1. ADC: Analog-to-digital converter.
2. ATT: American multinational telecommunications.
3. ALOFT: Airborne light optical fiber technology.
4. CPM: Cross-phase modulation.
5. DAC: Digital-to-analog converter.
6. IC: Integrated circuit.
7. MASER: Microwave amplification by stimulating emission of radiation.
8. MCI: Medical council of India.
9. OFT: Optical fiber technology.
10. OFC: Optical fiber communication.
11. OFN: Optical Fiber Networks.
12. PCM: Pulse code modulation.
13. POF: Polymer optical fiber.
14. RIP: Refractive index profile.
15. ROF: Refractive optical fiber.
16. SPM: Self-phase modulation.
17. SDM: Space division multiplexing.
18. TOF: Tailored optical fibre.
19. WTOF: W-tailored optical fiber.
20. OWTOF: Optimized W-tailored optical fiber.
21. FTTN: Fiber to the neighborhood.

22. FTTx: Fiber-to-the-x.
23. FLAG: Fiber Optic Link Around the Globe.
24. FCMS: Fiber cable management system.
25. FSO: Free space optical.
26. WDM: Wave division multiplexing.
27. IGI: Inverted graded-index.
28. PCG: polymer-clad glass.
29. CFDS: Centralized failure detection system.
30. US: United States.
31. LED: light emitting diode.

List of Parameters

1. a: Fiber core radius for the WTOF/OWTOF.
2. A: Optical fiber area for the WTOF/OWTOF.
3. A_0: Scaling constant of the WTOF/OWTOF.
4. C_Φ: Specific heat of the WTOF/OWTOF.
5. d: Diameter of the bending section of the WTOF/OWTOF .
6. D: Chromatic dispersion for the WTOF/OWTOF.
7. f: Regularly varying function.
8. F: Hot spot parameter for the WTOF/OWTOF.
9. h: Heat transfer coefficient for the WTOF/OWTOF.
10. H: Heat convection transfer coefficient for the WTOF/OWTOF.
11. k: Thermal conductivity of the WTOF/OWTOF.
12. l: Light intensity parameter on the WTOF/OWTOF.
13. $l_{extreme}$: Extreme laser intensity of the WTOF/OWTOF.
14. L: Slowly varying function for the WTOF/OWTOF.
15. l_o: Out put power intensity of laser source the WTOF/OWTOF..
16. l_p: Length of bent the WTOF/OWTOF section.
17. m: Tailoring parameter for the WTOF/OWTOF.
18. n: Refractive index profile of the medium for the WTOF/OWTOF.
19. n_0: Axial refractive index at an incident point on the surface of the WTOF/OWTOF.
20. N_0: Direction cosine of incident ray on the surface of the WTOF/OWTOF.
21. P: Optical power for the WTOF/OWTOF.

22. Q_{out}: heat loss to the exterior for the WTOF/OWTOF.
23. Q_{stored}: Stored heat in the WTOF/OWTOF.
24. r: Core radius of WTOF/OWTOF.
25. R: The optical signal mode field radius of the WTOF/OWTOF.
26. S_0: Chromatic dispersion slope at λ_0 for the WTOF/OWTOF.
27. t: Time along region bending of the WTOF/OWTOF.
28. T: Absolute temperature at a radial position of the WTOF/OWTOF.
29. T_{max}: Maximum axial temperature inside the core of the WTOF/OWTOF.
30. T_0: Ambient temperature in the neighborhood of the WTOF/OWTOF.
31. T_R: Environment temperature of the WTOF/OWTOF.
32. v: Index of variation of T on the OWTOF.
33. z: Normalized propagation distance of the WTOF/OWTOF.
34. Z: Longitudinal coordinate along the WTOF/OWTOF distance.
35. α: Tailoring parameter of the WTOF/OWTOF.
36. η: Normalized axial propagation distance with respect to core radius for the WTOF/OWTOF.
37. ρ: Normalized radial position with respect to the core radius for the WTOF/OWTOF.
38. σ: Absorption loss coefficient of the medium for the WTOF/OWTOF.
39. σ_s: Stefan-Boltzmann constant.
40. λ: Wavelength of the WTOF/OWTOF.
41. λ_0: Zero dispersion wavelength of the WTOF/OWTOF.
42. β_v: Volumetric thermic expansion coefficient of the WTOF/OWTOF.
43. φ: Electric polarizability thermic coefficient of the WTOF/OWTOF.
44. Φ: The density of the WTOF/OWTOF.
45. ϵ: Surface emissivity.

ABSTRACT

This research work studies the temperature effects in W-shaped core refractive index optical fiber. The work designs an optimized W-tailored optical fiber (OWTOF) that checks the effect of rising temperatures in W-tailored optical fiber (WTOF) for better communication. Initially, an introduction to the general concept of optical fibers including tailored optical fibers (TOF), temperature effects and models is presented as a background. This is followed by studies on existing literature on optical fibers where a gap is identified. The gap is that; **temperature rise in communication fibers is challenging the use of tailored fibers through unnecessary distortion and delay in information. Also, fiber design is limited in scope because of existing design practice**. Thus the need to optimize fibers for better communication. To fill in this gap, a three stage optimization process is designed and a methodology for achieving this optimization for the benefit of telecommunication systems and services is presented. Here, a regularly varying function is introduced in the geometry of WTOF for the temperature parameter leading to the design of the OWTOF. Finally, analytical and numerical simulations covering the performance of the OWTOF in relation to WTOF are stated and proven. Additionally, six research questions and remarks are answered. A major result of this work shows that the OWTOF is a better fiber for controlling temperature rises than the WTOF at a propagation distance around one unit. Hence, better suited for communication without distortion and delay compared to WTOF in this region. Finally, the research work concludes with three recommendations for improving this work for better communication.

Chapter 1

Introduction

1.1 Optical Fiber Technology (OFT)

Fibers are the principal load carrying component of a composite. The characteristics of a fiber influence the effective mechanical and damage properties of the composite fabricated from it. Fibers work on the principle of total internal reflection[1]. Optical fiber is defined as a thin flexible fiber with a glass core through which light signals can be sent with very little loss of signal strength. Optical fiber has a long thin strand about the size of human hair and is made up of a very pure glass. This strand is called the core of the optical fiber. Normally, light travels through the core of the fiber through a dark flexible material surrounding the core known as cladding. The clad reflects back any light that escapes the core. The outside of a clad contains a plastic coating called a buffer that protects the fiber from damage and moisture. Optical fibers have been widely used to guide laser energy for industrial, medical, civil and military applications. Commonly, thousands of optical fibers are placed together in one optical cable protected by an outside covering called a jacket for applications and

[1] Total internal reflection is defined as a phenomenon which occurs when light travels from a more optically dense medium (a medium with higher refractive index) to a less optically dense medium (a medium with lower refractive index) such as water to air

use. Optical fiber cable consists of a bubble of glass threads each of which is capable of transmitting modulated messages onto light waves from one place to another. Optical fiber cable works on the principles of reflection and refraction[2]. When light strikes a mirrored surface, it undergoes reflection. Additionally, when light travels between two media that are of different thickness or densities, it refracts depending on the angle at which it strikes the second medium. In physics, it is known that there is a certain angle whereby light no longer travels between the media. On the contrary, it gets reflected back into the original medium completely. The boundary at this point now acts like a mirror. This phenomenon is known as total internal reflection and is the basis of the optical fiber cable. When a light ray is sent into an optical fiber, it is sent at an angle towards the side of the fiber that will reflect. The light reflects and then strikes the opposite side of the fiber at an angle that will make total internal reflection possible. This light ray will travel through the whole length of the fiber. The angle of incidence to which the angle of refraction is 90 degrees is called the critical angle. Optical fiber cable equipped with the phenomenon of total internal reflection as in transmitters and receivers form the basis for optical fiber communication.

Optical fiber communication (OFC) refers to method of transmitting information from one place to another by sending pulses of light through an optical fiber. OFC investigates new generations of ultra-low-loss and isotropic where the light forms an electromagnetic carrier wave that is modulated to carry information. The OFC uses optimization technologies for current and efficient use of older fibers installed long time ago. They are also used in photonic systems for information processing and hybrid opto-electronic integrated circuits (ICs); Bechtel [8] as well as in sensors; Giallorenzi et al. [35]. OFC provides a rudimentary understanding of an optical fiber technology and applications in today's information world. Optical fiber technology

[2]By refraction, we mean a phenomenon where the wave direction changes the path from one medium to another caused by its change in speed and wavelength of the waves. Similarly, reflection can be defined as the change in the direction of a wave front at an interface between two different media so that the wave front returns into the medium from which it originated

(OFT) refers to the technology that uses glass to transmit data from one point to another. The OFT can be divided into two major fields; opto-telecommunication fibers and non-communication fibers. Opto-telecommunication for communications do not distort the signal and are resistant to external reactions while non-communication optical fibers are optimized individually for signal processing in a complex and usually preset way. OFT transports data from one area network to another point. It is as a result of this transportation tendency that OFT dominates large telecommunication industries.

1.2 Historical Development of OFT

The first optical fiber cable was the result of joint work between the Corning and Siemens Corporations. Corning provided the fiber technology and Siemens the cabling technology. Around 400 B.C., the Greek army used to send coded messages by reflecting light in flashes from one place to another using polished shields. Many modern navies to date use lantern signaling devices as a means of ship-to-ship communication. In the late 1800's, there were the advent of the telegraph and telephone which used wires to transmit signals. In the 1840's, the physicists: Daniel Collodon and Jacques Babinet showed that light could be directed along jets of water for fountain displays. Colladon designed a device for conservation of arts and science in Paris. In the 1850's the British physicist, John Tyndall performed a similar demonstration using water fountains. Tyndall demonstrated that light could travel through a curved stream of water and proved that a light signal could be bent. Additionally, Tendall proved the bending of light by setting up a tank of water with a pipe that ran out of one side. Tyndall demonstrated that light used internal reflection to follow a specific path by using a jet of water that flowed from one container to another and a beam of light. In 1880, Alexander Graham Bell invented a photo-phone. The photo-phone enables a person to speak via a microphone that causes a mirror to vibrate. The vibrating mirror would then reflect the sunlight in a pattern over open space. Graham Bell's telephone was proved to be more realistic than the first telephone. In that same year, William Wheeler assembled a system of light pipes lined with a highly reflective coating that illuminate homes by using light from an electric arc lamp. In 1888, physicians Roth and Reuss illuminated a human body cavities by bending glass rods. In 1925, John Logie Baird demonstrated the phenomenon of transmitting moving images leading to the invention of the television.

During the 1930's, Heinrich Lamm successfully transmitted images through a bundle of fibers. The images were those of a light bulb filaments to look inside the human body. In 1938, Alec Reeves conceived the idea that telephone signals could be converted into digital signals for efficient transmission and then back into analog form for delivery. This system is known as Pulse Code Modulation (PCM). The amplitude of an analog signal is periodically sampled and the sample translated into a digital binary code. In 1950s, an optical fiber technology experienced a phenomenal rate of progress leading to the development of the fiberscope. In 1951, Holger Moeller applied for a Danish patent on optical fiber imaging in which he proposed cladding glass with a transparent low-index material. Unfortunately, Moeller was denied because of Baird and Hansell's patents.

In 1952, United Kingdom physicist Narinder Singh Kapany invented the first actual optical fiber cable based on John Tyndalls experiments. Additionally, Charles Townes and his colleagues developed a microwave amplification by stimulating emission of radiation (MASER). In 1956, Narinder Kapany and his colleagues coined the term optical fiber at the Imperial College of Science and Technology in London. Generally, glass fibers experienced excessive optical loss due to loss of light signals as it traveled through the fiber thus limiting transmission distances. In 1958, the laser which was an efficient source of light was introduced. Charles Townes and Arthur Schawlow intended to show that lasers could operate in optical where light will be reflected back and forth to generate amplified light. In 1960, the operating heliumneon gas laser was invented and tested by using a synthetic pink ruby crystal. Elias Snitzer of American Optical published a 1961 theoretical description of a single mode fiber having a core so small but can carry light with a single waveguide mode. Elias demonstrated how a laser directed through a thin glass fiber will have implications in medicine. Unfortunately, it lost too much light energy to have any communication application. In 1964, Charlse Kao published a paper demonstrating that light lost in a glass fiber could be decreased dramatically by removing some impurities. Koa further discovered that attenuation of an optical fiber is caused by some impurities. In 1970, Maurer developed a glass fiber that exhibited attenuation at less than 20 dB/km. The United States (U.S) military moved quickly to use Koa optical fiber for improved communications and tactical systems. In 1976, U.S. Air Force developed her Airborne Light Optical Fiber Technology (ALOFT) program. The ALOFT program had much cheaper operating costs.

In 1979, American multinational telecommunications (ATT) installed a public demonstration system in Lake Placid and New York which was used with great success carrying multiple television signals. In 1983, U.S. medical council of India (MCI) company working with Corning opened a commercial optical fiber cable system between New York and Washington. An optical fiber transmission was digitized for increasing quantity of digital computer data being sent over the world's telephone lines. In 1986, Desurvire developed an erbium-doped fiber amplifier which reduced the cost of long-distance systems. In 1988, the first transatlantic telephone cable went into operation which utilizes Desurvires laser amplification technology.

In 1991, Desurvire demonstrated optical amplifiers that were built into an optical fiber cable. The all optical system could carry 100 times more information than cable with electronic amplifiers. The photonic crystal fiber was developed which guides light by means of diffraction from a periodic structure therefore improving performance. In 1996, the first optical fiber cable that uses optical amplifiers was laid across the Pacific Ocean. Fiber Optic Link Around the Globe (FLAG) became the longest single-cable network in the world providing infrastructures for the next generation of Internet applications. An Optical fiber for applications outside the trunk transmission field are known as specialty or tailored optical fiber (TOF) Romaniuk and Wjcik [27]. TOF can be divided into two major fields; opto-telecommunication fibers and non-communication fibers. Opto-telecommunication fibers are used for telecommunication purposes. An example of such fiber is the W-tailored optical fiber.

1.3 W-Tailored Optical Fiber

W-Tailored optical fibers are fibers of specialty that are used in tailing and compensating dispersal in optical communication fibers. Such optical fibers have W-shaped core design. Additionally, they have four basic affecting parameters called the index tailoring parameter, core radius, core absorption coefficient and intensity of light launched to the fiber core. Mohamed et al. [14] remarked that due to significant reduction of heat loss in optical fibers of specialty, the possibility of using them in the field of communications increases. However, the energy transmission capacity is to be defined by the input power that raises the temperature of the fiber to the maximum acceptable level. Refractive optical fibers (ROF) distinguishes several fundamental classes of refractive index profiles (RIPs) in a TOF of specialty. The RIPs are analogous to the classes for OFC and include: step-index, gradient-index, monotonic and non-monotonic profiles. Examples of such profiles include; W-profiles, ring-index, multi-ring-index. Distant RIPs differ considerably in diameter, sensitivity to micro bending and their modal structure. The introduction of a complex RIP in an optical fiber is to optimize the dispersion in terms of flattening. This optimization process is connected with optimizing parameters such as cut-off point, shaping of field radiation characteristics and coupling capabilities with other fibers. In this research work, optimization of WTOF is carried out. The effects of dimensioning the radial position of the fiber core on the maximum axial temperature of WTOF is studied and presented.

1.4 Temperature Rise in WTOF

Temperature is a degree or intensity of heat present in a body. There exists three forms of temperature in WTOF namely; ambient temperature, absolute temperature and maximum axial temperature T_{max}. It is known in fiber optics that increase in any of the above mentioned temperature causes fiber degradation which in turn affects information and communication quality of experience. Temperature rise in fibers can lead to high optical powers propagating in regions with small bending diameters. Additionally, when the bending diameter is small, temperature increases in time (see figure 1.1). In smaller diameters, a part of the optical signal transferred (packet of information) from the core to the surrounding cladding and coating losses content due to temperature rise (T_{max}) of a core fiber. In case of the absolute temperature on high bending diameters, it is shown that absolute temperature fluctuates in time along a propagation path. Relative to communication flow, this temperature effect leads to degradation of the protection layers of the fiber with the consequence of possible rupture and fusion effect ignition (see figure 1.3) in the fiber core; Andre et al. [21] (see figures 1.2, 1.4 and 1.5). The temperature rise has an increasing effect

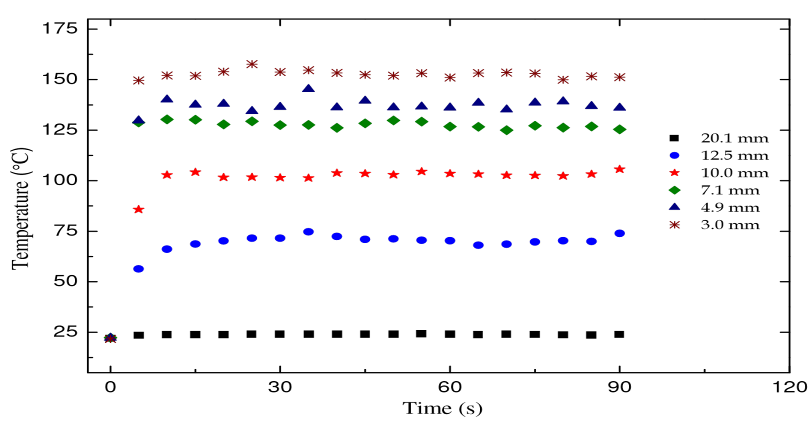

Figure 1.1: **Temperature in the bent region along time; Andre et al. [21]**

on the optical power at low bending diameters; see figure 1.2. The implication of temperature rise in WTOF is that, it can lead to rupture and fusion effects which in turn degrades the fiber via injected power losses and distort or delay communication. Thus there is need to further still model temperature rise in WTOF especially the absolute and the T_{max} to improve communications.

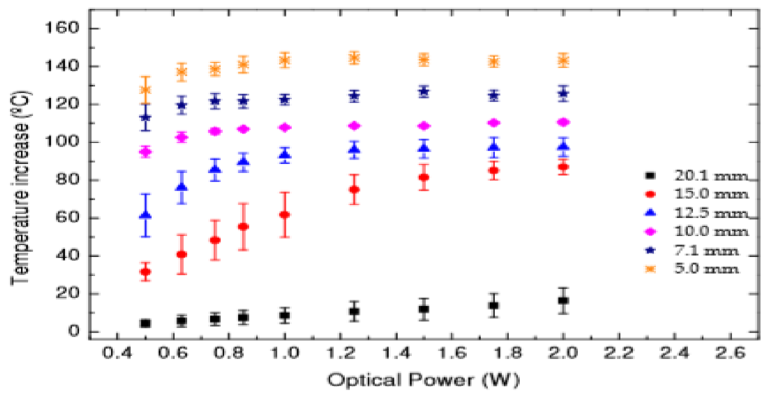

Figure 1.2: **Temperature increase on optical power; Andre et al. [21]**

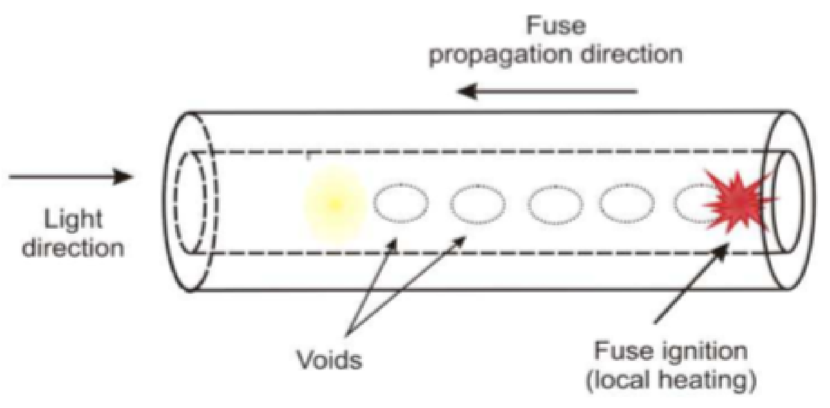

Figure 1.3: **The fuse effect in an optical fiber; Andre et al. [21]**

1.5 Temperature Models in WTOF

In the recent years, there exists several substantial development of theoretical models for the fiber fuse phenomenon; Andre et al. [21]. Andre et al. [21] constructed a temperature model that transferred the optical signal energy to non guided modes by

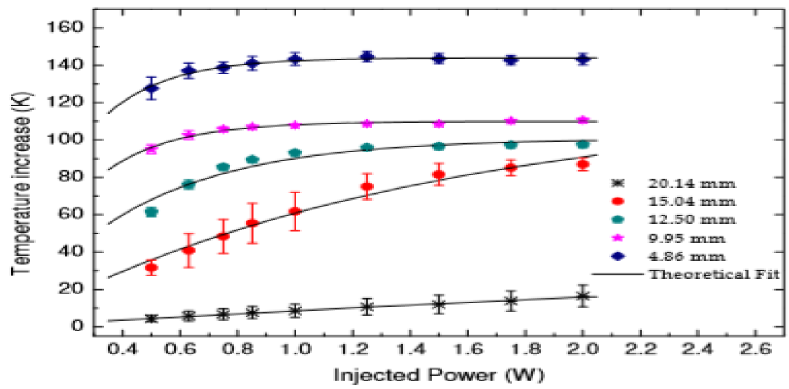

Figure 1.4: **Temperature increase and injected power; Andre et al. [21]**

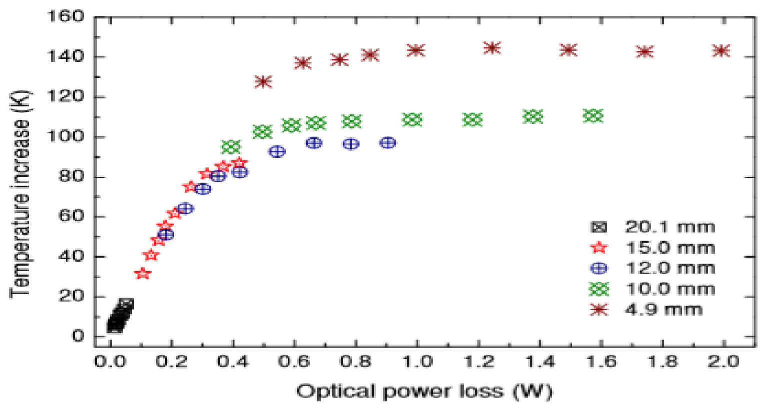

Figure 1.5: **Temperature rise and optical power loss; Andre et al. [21]**

observing the acrylate layer into heat. The model is given by:

$$\frac{dT}{dt} = \frac{Q_{stored}}{\Phi C_\Phi A l_p}, \tag{1.1}$$

where Q_{stored} is given by:

$$Q_{out} = \pi d l_p h(T - T_0), \tag{1.2}$$

d is the diameter of the fiber bent section, T_0 is the ambient temperature, A is the optical fiber area and Φ is the density, C_Φ is specific heat of the fiber, T is the absolute temperature and t is time along region bending. Rocha et al. [3] modeled the fuse effect by a one-space-dimensional heat conduction equation coupled with the optical power evolution along the fiber length. The model is given by:

$$\Phi C_{\Phi}\frac{\partial T}{\partial t} = k\frac{\partial^2 T}{\partial Z^2} + \frac{\alpha P}{\pi R^2} - \frac{2\sigma_s \epsilon}{R}\left(T^4 - T_R^4\right), \tag{1.3}$$

$$\frac{dP}{dZ} = -\alpha P, \tag{1.4}$$

where $T(t, z)$ is the fiber temperature, P is the optical power, Z is the longitudinal coordinate along the fiber distance, k is the thermal conductivity of the fiber and R is the optical signal mode field radius. However, the second term of the heat conduction equation is the heat source caused by light absorption where $\alpha(T)$ is the local absorption coefficient, σ_s is the Stefan-Boltzmann constant, ϵ is the surface emissivity and T_R is the environment temperature. In another work, Andre et al. [23] shows that the chromatic dispersion slope variation with temperature as a function of the zero dispersion wavelength is given by:

$$\frac{\partial n}{\partial T} = \frac{(n^2-1)(n^2+2)}{6n}\left(\varphi - \beta_v\right), \tag{1.5}$$

where β_v is the volumetric thermic expansion coefficient, n is the refractive index profile of the medium and φ is the electric polarizability thermic coefficient.

Hamp et al. [18] has shown that temperature and chromatic dispersion are related by:

$$\frac{\partial D}{\partial T} = \frac{1}{4}.\left(\lambda - \frac{\lambda_0^4}{\lambda^3}\right).\frac{\partial S_0}{\partial T} - \frac{S_0.\lambda_0^3}{\lambda^3}.\frac{\partial \lambda_0}{\partial T}, \tag{1.6}$$

where temperature has a positive variation with the chromatic dispersion.

Recently, Mohamed et al. [14] modeled a single mode (SM) optical fiber that investigated the thermal effects in W-shaped optical fibers carrying high power as in military and medical applications. Mohamed et al. [14] aimed to minimize temperature rise inside the fiber core by selecting suitable values for the affecting parameters namely; the index tailoring parameters, core radius, core absorption coefficient and intensity of light launched to the fiber core. The laser beam is transmitted through a medium and a portion of its internal energy is absorbed by the medium. Moreover, the internal energy heats the surrounding medium and changes the internal energy along the laser path. The redistribution of the internal energy are resulted from the changes that occur in both direction of propagation distance and normal to it. Those laser beam are assumed to have a Gaussian distribution of the undistorted intensity given by:

$$l(\rho, z) = \frac{l_0}{F^2} exp\left(-\sigma z - \frac{\rho^2}{F^2}\right), \tag{1.7}$$

where z is the propagation distance, l_0 is the output power intensity of laser source, F is the hot spot parameter and ρ is the normalized propagation distance. Furthermore, the initial conditions for undistorted intensity equation are given by $F|_{z=0} = 1.0$ and $\rho|_{z=0} = \rho_0$. Mohamed et al. [14] represented the maximum axial temperature T_{max} as a critical factor in the thermal effect of WTOF as:

$$T_{max} = T_0 + 0.5A_0 \left(0.5\rho^2 + \frac{\rho k}{Ha}\right). \tag{1.8}$$

Where T_0 is the ambient absolute temperature and σ is the absorption of the medium, scaling constant A_0 is such that:

$$A_0 = \frac{\sigma l_0 a^2}{k} \left(\frac{\rho_0}{\rho}\right)^2 exp(-2\sigma a N_0 n_0 \eta), \tag{1.9}$$

where H is the convection heat transfer coefficient and a is the fiber core radius, where l is the intensity of light launched to the fiber core, N_0 is the direction cosine of the incident ray and n_0 is the axial refractive index at any incident point.

1.5.1 Observation on Existing Temperature Models

In the temperature models discussed above, it is clear that the rise in temperature will continue to be experienced in WTOF since the models are transient models. Transient temperature models give room to temperature rise in time and space. Unless a better time resistant temperature model is designed, the problem of distortion and delay originating from fuse effects, rupture effects and so on will put the future of communication at stake. Communication at stake means security, business and medical threats. Thus, the need to optimize WTOF for better communication services via temperature minimization principle.

1.6 Statement of the Problem

Despite advancements in OFT for telecommunication purposes today, the effect of heat in W-shaped core refractive index optical fibers is a great challenge. For instance, it is well known that heat increases the maximum axial temperature of the core leading to certain communication effects. The effects on the core are both natural and artificial. The natural effects may include phase transition temperature rise and glass transition temperature rise. Both effects can lead to change in dimension of communication from originally transmitted communication to a distorted communication. Suppose a telecommunication service user sends a message when the core of the fiber experiences a temperature rise. Under this temperature rise condition in time, the core experiences a change in dimension (see figure 1.1) which shrinks the core together with the packets of information sent. The message reaches the receiver in a shrink form. The shrink message reaches the receiver with lost power packets (see figures 1.2, 1.4 and 1.5) of information yielding misinterpretation and misunderstanding capable of causing confusions and contradictions via the fuse effect (see figure 1.3). Second, artificial effects are caused by the redistribution of internal energy due to temperature variations leading to unnecessary delays in communication. Suppose a telecommunication user wants to make an urgent call when the internal energy of the core is raised due to rise in temperature. Under this condition, the T_{max} of the core fiber will exceed the normalized temperature gradient. This is sequel to the direct relationship between energy and temperature. The more the energy redistribution, the more the rise in temperature above the normalized maximum for communication. The message waits for a certain time until the energy redistribution falls to the normalized communication limits. This waiting time is called the delay time. The total delay is the sum of all the delays arising from the energy redistribution forcing temperature rise outside the acceptable region. The stored energy increases in time (see equation 1.1). Also, the conductivity of the fiber material is degraded (see equation 1.3) as a result of the degradation of the thermal effects (see equation 1.5). Chromatic dispersion occurs each time energy is redistributed as in equation 1.6. The resulting impact is the inability of the user to solve urgent call problems when communication is via WTOF with temperature models transient in nature. This is because such fibers are open to the fuse effects, rupture effects, chromatic dispersion effects due to temperature rise. It is then imperative to design temperature models that regulate the effect of heat leading to temperature rise in WTOF for better communication.

1.7 Aim of the Research

The aim of this research work is to design optimized temperature model for WTOF that is capable of stabilizing the thermal effects leading to temperature rise in the core to minimize chromatic dispersion effects, rupture effects and fuse effects that result in distortions and delays in communication.

1.8 Objectives of the Research

1. To formulate optimization strategies that can minimize temperature rise in the core of WTOF.

2. To design functional models that regulates temperature rise in WTOF.

3. To test the functional models designed in two (2) above and compare the performance of functional models with those existing in the literature.

1.9 Research Questions

1. What are the conditions for optimizing the T_{max} of a WTOF?

2. What analytic function is suitable for designing an optimized WTOF strong enough to regularize the T_{max}?

3. How can the optimized WTOF behaved in performance relative to the existing WTOF?

4. Suppose a telecommunication service user sends a message when the core of the fiber experiences a temperature rise. What is the expected fuse effects on WTOF and optimized WTOF?

5. Suppose a telecommunication user wants to make an urgent call when the internal energy of the core is raised due to rise in temperature. What is the expected rupture effects on WTOF and optimized WTOF?

6. Suppose a telecommunication user wants to make an urgent call when the internal energy of the core is raised due to rise in temperature. What is the expected chromatic dispersion on WTOF and optimized WTOF?

1.10 Significance of the Research

This research is significant to the following category of persons:

1. Government willing to upgrade OFT within her domain.

2. Academics as a source of reference.

3. Telecommunication companies willing to provide better services to customers.

1.11 Scope and Limitation of the Research:

The research covers OFT based telecommunication fibers. However, results may be weak for OFT of non communicating type.

1.12 Definition of Terms:

Definition 1 (Fibers) *Fibers are defined as the principal load carrying component of a composite.*

Definition 2 (Optical Fiber) *An optical fiber is defined as a thin flexible fiber with a glass core through which lights signal can be sent.*

Definition 3 (Optical Fiber Cable) *An optical fiber cable is a bubble of glass threads each of which is capable of transmitting message modulated onto light waves from one place to another.*

Definition 4 (Optical Fiber Communication (OFC)) *An OFC is a method of transmitting information from one place to another by sending pulses of light through an optical fiber.*

Definition 5 (Optical Fiber Technology (OFT)) *An OFT is a technology that uses glass to transmit data from one point to another.*

Definition 6 (Tailored Optical Fiber (TOF)) *TOF is a special generation of optical fiber waveguides (glass or polymer) that transmit optical signals for communication purpose.*

Definition 7 (W-Tailored Optical Fiber) *W-tailored optical fiber (WTOF) is that TOF with a W-shaped core for communication purposes.*

Definition 8 (Temperature) *Temperature is a degree or intensity of heat present in a body.*

Definition 9 (Refractive Index) *The refractive index at a boundary between two media is the ratio of the sine of the angle of incidence to that of the sine of the angle of refraction.*

Definition 10 (Atmospheric-Turbulence) *Atmospheric-turbulence is a random phenomenon which is caused by variation of temperature and pressure of the atmosphere along a propagation path.*

Definition 11 (Angle-Of-Arrival Fluctuations) *Angle-of-arrival fluctuations is the laser beam wavefront arriving at the receiver will be distorted due to the presence of turbulence in the atmosphere which leads to spot motion or image dancing at the focal plane of the receiver.*

Definition 12 (Dispersion) *Dispersion is the phenomenon in which the phase velocity of a wave depends on its frequency.*

Definition 13 (Attenuation) *Attenuation is the reduction of signal strength or light power over the length of the light-carrying medium. Fiber attenuation is measured in decibels per kilometer.*

Definition 14 (Pulse Code Modulation (PCM)) *The PCM is the process of converting an analog signal into a* 2^n*-digit binary code.*

Definition 15 (Fiber Fuse) *Fiber fuse is a phenomenon that results in a specific type of catastrophic destruction of an optical fiber core from the point of initiation toward the laser light source.*

Chapter 2

Literature Review

An optical fiber is a long, thin strand of very pure glass about the size of a human hair. Optical fiber guides light through concentric layers of the core, cladding and coating. The core of an optical fiber has a central section made of silica. The cladding of an optical fiber is a silica layer around the core. It creates an optical waveguide which confines light in the core by the phenomenon of total internal reflection at the interface of the core-cladding. Optical fibers are arranged in bundles called optical fiber cables and are used in transmitting signals over long distances with the help of bubble of glass threads within the cable. The bubble of glass threads transmits messages modulated onto light waves from one place to another via optical fiber technology (OFT). OFT is a significant discipline of science and technology that deals with information and telecommunication technology. OFT consists of two fundamental areas namely; telecommunications and non-telecommunication optical fibers. An optical fiber for telecommunication may have some distortion tendency which in turn can change the dimension of communication. The non-telecommunication optical fibers are not used in communication. The two fundamental areas above together with other related areas of technical sciences formed a widening discipline known as opto-electronics and photonics. OFT devices transmit data from an optical fiber network area to another.

2.1 Optical Fiber Networks (OFN):

Research work covering OFT is dominant in the literature. For instance, Tkach [28] studied the challenges of scaling in optical fiber networks (OFN) and proffered some solutions using optical parallelism method leading to the faster growth rates of router interface in optical fiber networks of around 40 to 60 percent. Chraplyvy [2] studied spectral efficiency limits in OFN. By using the method of logarithmic scaling of transmission distance, it was shown that fiber capacity limit depend moderately on the transmission distance. Morioka [36] studied the rebirth of coherent detection in OFN and its super channels. Using the methods of digital-to-analog converters (DACs) and analog-to-digital converters (ADCs), it was shown that one can enable the capabilities of digital electronic signal processing in OFN. Essiambre and Tkach [25] studied the capacity trend limits of optical communication. Using the method of transmission waveguides such as multicore or few-mode optical fibers resulted into yielding cost saving both in capital and operating expenditure. Friis and Sigmund [17] studied the topology optimization of optical surfaces. Using the method of a systematical design, a higher robustness that considered practical dimensional tolerances is constructed. Richardson [6] outlined the factors that drive the adoption of space division multiplexing (SDM) in future optical networks. Individual optical transport systems method was used. It was shown that placing the optical transport system helps in keeping cost and energy consumption per bit constant in OFN. Singh and Singh [31] studied the nonlinear effects in optical fiber that occur due to inelastic - scattering phenomenon. Using self-phase modulation (SPM) and cross-phase modulation (CPM), substantial increase in the absolute value of the power carried by a fiber to allow systems to trade off capacity for transmission reach in real time in a software-defined manners were obtained. Peng et al. [9] studied the fabrication and characterization of polymer optical fiber (POF) and prospects of POFs. The characterization was obtained by investigating the sensor design and system architectures methods for various applications based on perfluorinated polymer. It was obtained that graded-index POF increases the bandwidth of tailored index profile of optical 'fibers. OFT is dominating the market from a long time due to its high data rate, long distance transmission capability. In this regard, Kokaje et al. [22] reviewed the recent development of OFT and outlined areas of OFT developed in the last decade including certain management procedures. From the above, it is clear that the place of management in optical fiber technology cannot be over emphasized. .

2.2 Fiber Management System:

There has been an increasing development of fiber cable management system (FCMS). For instance, Kumar and Bhatt [30] studied cable fault management networking leading to networks inability to start normally. Using the method of splicing to control fiber breaks in cables, it was shown that splicing is a good management process. Ramamurthy et al. [32] studied survival of wave division multiplexing (WDM) mesh networks. By using fault detectors leading to higher bandwidth of fiber cable networking, a better option that manages high speed internet surfing was obtained. Ramamurthy and Mukherjee [33] reviewed fault management in WDM mesh networks, basic concepts and research challenges. It was shown that software and optical ring network methods as a fiber cable fault management procedures are higher cost-effective procedures that provide the best cable management, flexibility and growth capabilities. Rahman and Ng [19] studied the centralized failure detection system (CFDS) in scan networks. Using MATLAB-based graphical user interface, a network design that shows the far end loss of a particular station in the fault location was provided. In recent years, fiber cable management system together with free space optical (FSO) communication has gained significant importance owing to its unique features of large bandwidth and high data rate. FSO communication uses optical carrier in the near infrared (IR) band to establish either terrestrial links within the Earths atmosphere or inter-satellite/deep satellite links. However, despite its great potentials, its performance is limited by the adverse effects including absorption, scattering and turbulence in the atmosphere.

2.3 Optical Fiber Challenges

Kaushal et al. [11] studied associated problems connected with optical communication in space and proffered solutions. The method of orbital angular momentum was used. It was obtained that utilizing the high capacity of optical carriers in case of space-based and near-Earth optical communication links is a good solution. Ghassemlooy and Popoola [40] studied terrestrial challenges in FSO communications. Mitigation techniques leading to improvements in the performance and availability of FSO systems were provided. The techniques are as in figure 2.1 below.

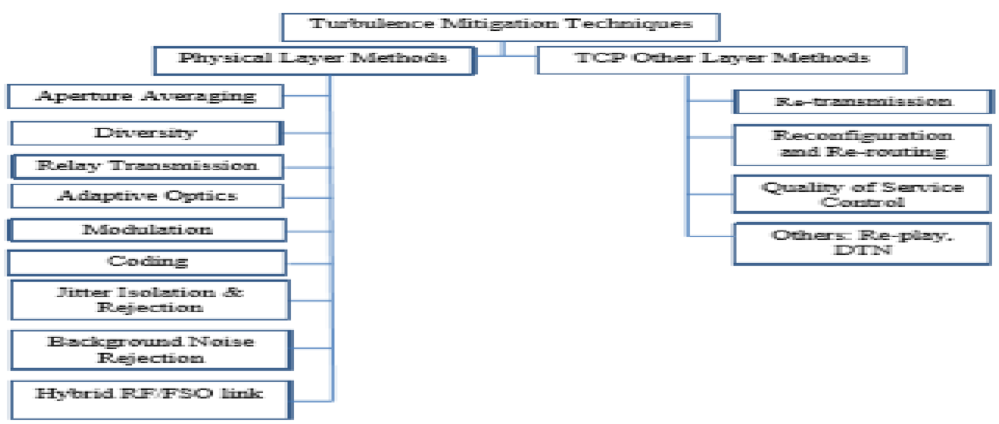

Figure 2.1: **Turbulence mitigation techniques; [40]**

Hemmati [10] surveyed the deep space optical communication challenges. Details of this process are as in figure 2.2 below.

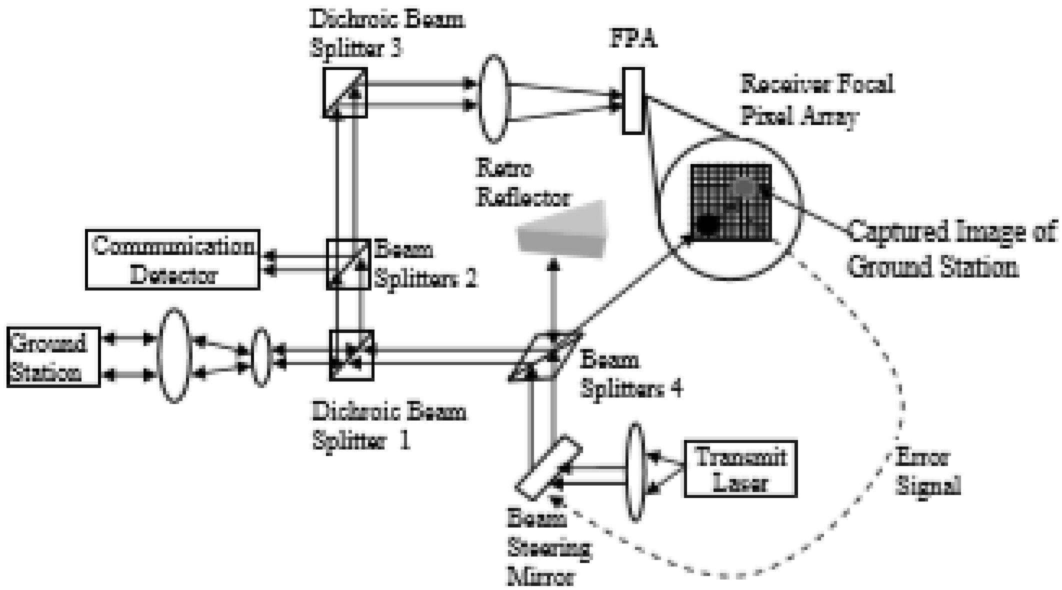

Figure 2.2: **The basic concept of ATP for FSO communication system; [10]**

From figure 2.2, it is clear that optical communication in space mitigation techniques and OFT are important areas of science and economics. Together with related areas of technical science, the field of tailored optical fibers was found. Tailored optical fibers are divided into two major sub-fields which includes opto-telecommunication and non-communication fibers.

2.4 Tailored Optical Fibers (TOFs):

By TOFs, we mean a special generation of optical fiber waveguides (glass or polymer) processing and transmitting optical signals for communication purposes. Recently, several types of TOFs have emerged. Examples of these emerging TOFs are the W-tailored optical fiber, M-tailored optical fiber, V-tailored optical fiber and so on.

The literature covering TOFs is rich. For instance, Thienpont et al. [12] studied the design of axisymmetrical tailored concentrators for light emitting diode (LED) light source applications. A differential equation for solving tailored compound parabolic concentrator (CPC) related problems was derived. The principle covering CPC device in non-imaging optics was tested and collected. The collection of 72 % ideal reflective coating presumed from CPC was obtained. Kask et al. [13] studied a silica-based optical fiber with refractive-index profile tailored in a region of 1.45 - 1.62 for fiber-optic chemical detection. By using multimode large-core inverted graded-index (IGI) fiber and polymer-clad glass (PCG) fiber, it was obtained that the tailoring of detection sensor for refractive indexes of the fiber was improved. Raack et al. [5] reviewed the cost-optimal deployment of optical access networks by considering variants of the problem of fiber to the neighborhood (FTTN). It was shown that the construction unified integer programming model has the capacity to combine all sub-models of fiber-to-the-x (FTTx) problems.

2.5 Optimizing TOFs:

Mohamed et al. [14] studied the axial temperature distribution in WTOF's. By using single mode (SM) optical fiber, the thermal effects in W-shaped core refractive index optical fibers were investigated. It was obtained that the effects of the T_{max} variation of 49.8881 ^0C with η at $\alpha = 0.1$ inside the fiber core was minimized. Cohen et al. [20] studied photon-pair generation in tailored optical fibers. Using the method of designed dispersion, the result shows that photon pairs with no spectral correlations can be produced and be directed in pure-state wave packets without filtering. Engeness et al. [34] applied the method of dispersion-tailoring of omniguide and other photonic band-gap guided fibers such as transerverse electric TE01 based on weak interactions. It was obtained that, the immune of the non degenerate TE01 was improved. Manceau et al. [15] studied the terahertz pulse emission optimization for tailored fibers on air. Using spatial distribution of the electron density in the plasma string generated by the filament, the shortening of considerable terahertz pulse when the plasma string is tailored to a uniform density profile was obtained. Jiang et al. [41] studied the tailoring dispersion for broadband low-loss optical metamaterials using deep-sub wavelength inclusions. By designing a metamaterial dispersion that is controllably tailored across negative, zero and positive refractive index values. It was obtained that experimentally accessible deep-sub wavelength inclusions to a simple metal dielectric fishnet structure can be improved. Wang et al. [7] studied the robustness of photonic crystal waveguides with tailored dispersion properties. A novel waveguide design with two different constant group index waveguide regions was proposed. Additionally, an illustration of efficiency robust optimization formulation was obtained. The formulation indicates that topology optimization procedure can provide a useful tool for designing waveguides for tailored optical fibers. Yang et al. [4] applied the construction method of tailored facets in free form reflectors. Using ray tracing through third order 2D Bzier curves, the result shows that four corners that are coplanar can be produced. Tripathy et al. [29] surveyed approaches of the design of a novel macromolecular system with tailored optical properties. The aim is to review the behavior of growing large single crystals that have desirable mechanical and thermal stability. Using solvatochromism technique, the molecular hyper-polarizability was determined. Romaniuk and Dorosz [26] studied the measurement techniques of tailored optical fibers that have non-standard geometrical shapes and dimensions. Using refractometry and polarimetry, it was obtained that the characterization and measuring methods of TOFs have to be standardized to enable the designers of the photonic functional systems to apply them in a reliable and repeatable way. The tools are used for standardized, networked TOFs analysis is as shown below in figure. 2.3.

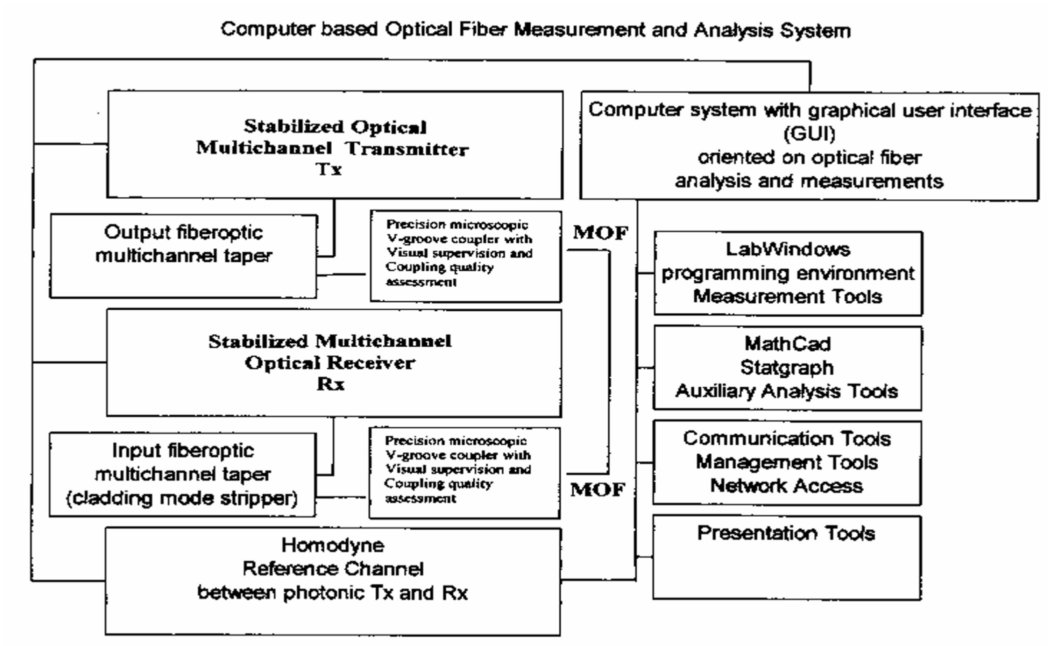

Figure 2.3: **Computer based optical fiber measurement and analysis system; [26]**

2.6 Literature Gap:

From the literature reviewed, it can be seen that a lot of works on OFT exist. Additionally, works on tailored optical fibers has been carried out. However, the problem of temperature rise in W-tailored optical fibers persists to date. This is even with the level of advancement in TOFs technology. From the literature, it is evident that temperature rise manifests in T_{max} parameter of existing W-shaped optical fiber. Visible effects include distortions and delays of communication. In the light of these effects, this thesis observed that

1. No WTOF that is capable of stabilizing the thermal effects leading to temperature rise exists; Mohamed et al. [14]. That is why the problem of communication delays and distortions are experienced even with the advancement of dubbed OFT to date. The thesis posits that WTOF with high maximum temperature

rising tendency cannot be optimally better than one where the temperature is slowly varying at an infinity index of temperature variation. Additionally, WTOF design that steadies the problem of regular variation of temperature is without doubt a better fiber than the existing WTOF fiber.

2. Generally, in material engineering, it is known that design precedes control equations. The case where governing equations are created first before control material designs are scarce in the literature. This approach requires functions as parameters within a domain of application and design. This limits TOFs to the industry for reasons to do with finance and machinery. To the best of our knowledge, such reverse process do not exist in the literature.

3. For the existing WTOF, temperature models are transient. It is known that transient models for an engineering application make the application transient also. This stands for the reason why existing WTOF lacks the requisite energy to withstand temperature excesses of time bound phenomena threatening communication.

This research work contributes to the literature of WTOF technology by filling the three gaps identified above. The research provides stabilizing conditions for constructing such functionally limiting temperature models as panacea to constructing and realizing such a fiber. Additionally, test results are presented for material construction. Finally, recommendations leading to ease of upgrading are provided. In chapter 3, we provide a methodology for designing such OWTOF.

Chapter 3

Methodology

3.1 Objective 1: Optimization strategies

Consider a WTOF laid in an environment Y whose thermal effects are due to the values of its (T), T_0 and T_{max} as in figure 3.1 below. The temperature T is measured

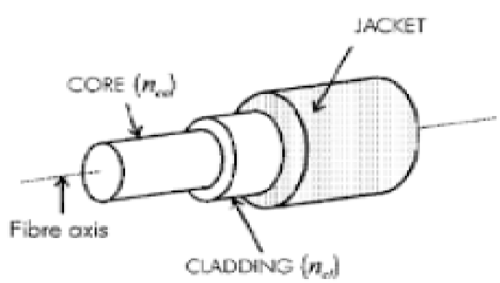

Figure 3.1: The structure of WTOF

Figure 3.1: **The structure of WTOF;**

from the exterior environment to the fiber environment. T_0 is the value of T within the immediate fiber environment. Finally, T_{max} is the value of the T in core of fiber to the cladding axis. For this fiber in question, it is known that the T_{max} is given by (1.8). As in section 1.6, T_{max} is an increasing function because of its transient nature. This implies that T_{max} keeps increasing in time whenever there is a change in the size of any affecting parameter. Consequently, there is need for optimization. To optimize the WTOF in figure 3.1, a three stage optimization strategy with basic architecture as in figure 3.2 below is constructed

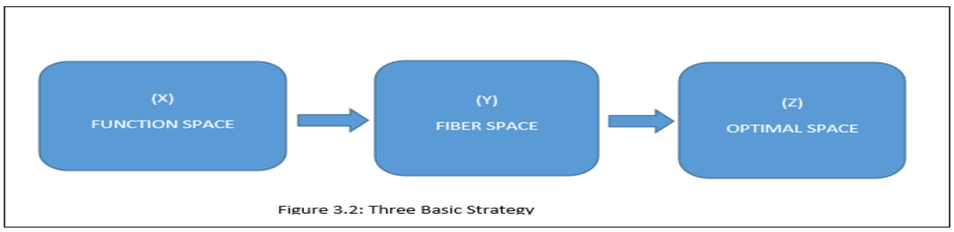

Figure 3.2: **The three stage optimization strategy;**

Broadly, the optimization strategy process involves identification and selection of a suitable analytic function in X out of many feasible functions in X equipped with requisite properties to minimize T in the fiber space Y onto the optimal space Z. The second stage involves identification of suitable projections of the fiber space Y onto the optimal space Z. The last stage involves interpretation of the optimal behavior of optimized functions embedded in Z in terms of their capacity to control thermal effects as manifested in the three temperature identified in section 1.4 above. Figure 3.3 below gives a detailed description of the specific optimization strategy constructed to control the temperature rise in WTOF presented in figure 3.1 above for better communication.

3.2 Objective 2: Model Design

To design the temperature model for the WTOF presented in figure 3.1 with the optimization strategy process as in figure 3.3, the following basic assumption on the fiber in question are made. These assumptions are those to do with light entering the

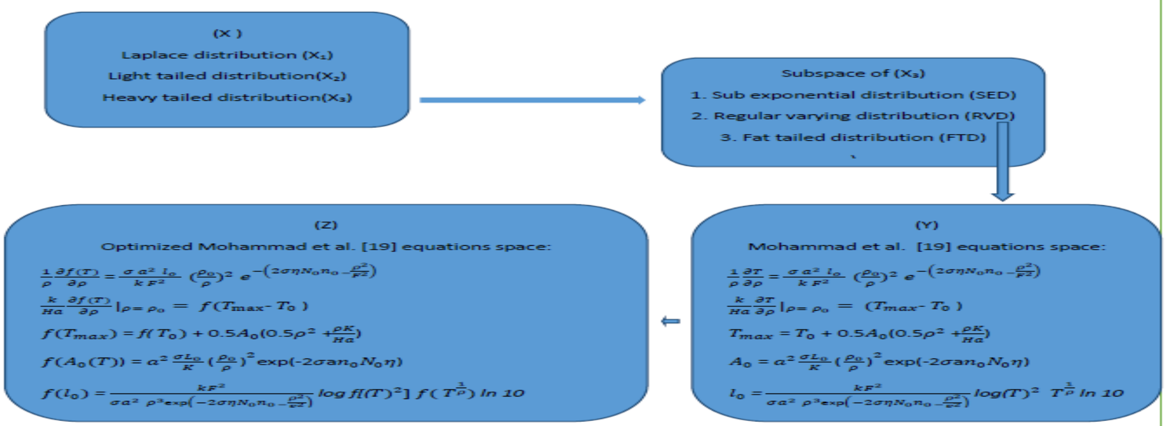

Figure 3.3: Optimization Strategy Process.

Figure 3.3: **The optimization strategy process;**

fiber, normalized radial position, tailoring index, core radius and intensity of light passed onto the fiber core as drivers of the thermal effects.

3.2.1 Basic Assumptions:

Consider an optimization problem to do with the T_{max} inside the core of a W-shaped optical fiber in figure 3.1. Suppose that light rays enter the core cladding region of the fiber at a ρ such that an arbitrary ray moving from air to the region satisfies the ray equation in Okoshi and Oyamoda [37]. Given that the core radius $r : r = \rho a$ where fiber core radius $a : a \in \Re$. Also, the normalized propagation distance $z : z = \eta a$. It is as given that a ray of light entering the core is a function of r, z and the launching conditions as specified below:

$$\frac{\partial^2 \rho}{\partial \eta^2} = \frac{1}{2n_0^2} \frac{\partial n^2}{N_0^2\, \partial \rho}. \tag{3.1}$$

Additionally, n is the refractive index profile of the medium given by:

$$n(\rho) = n_0 \sqrt{1 - 2\alpha\rho^2 + 2m\alpha\rho^4}, \tag{3.2}$$

where α and m are tailoring parameters, see Mohamed et al. [14]. If (3.2) is substituted in (3.1), simplified and the right hands side of (3.1) partially differentiated, then one obtains that:

$$\frac{\partial^2 \rho}{\partial \eta^2} = \frac{1}{N_0^2}\left(4m\alpha\rho^3 - 2\rho\alpha\right). \tag{3.3}$$

Let $\rho = \frac{\rho_n}{\sqrt{2m}}$ and $N_0 = \eta\frac{\sqrt{2m}}{\eta_n}$. By substituting for N_0 and ρ in (3.3) and simplifying yields:

$$\frac{\partial^2 \rho_n}{\partial \eta_n} = \frac{\eta_n^2}{\eta^2}\left(\rho_n^3 - \rho_n\right), \tag{3.4}$$

additionally, letting $\frac{\eta_n}{\eta} = 1$ and re-arranging (3.4) yields:

$$\frac{\partial^2 \rho_n}{\partial \eta_n} + \rho_n - \rho_n^3 = 0. \tag{3.5}$$

Equation (3.5) provides the partial change of the ρ with respect to the η. Let T denote the absolute temperature at ρ for an arbitrary WTOF. In view of Nowacki and Sneddon[39] and Smith [24] for this class of fiber, we have:

$$\frac{1}{\rho}\frac{\partial}{\partial \rho}\left(\rho\frac{\partial T}{\partial \rho}\right) = -\frac{\sigma l_o a^2}{kF^2}\left(\frac{\rho_0}{\rho}\right)^2 exp(-2\sigma n_0 N_0 \eta - \frac{\rho^2}{F^2}). \tag{3.6}$$

Under (3.6), Mohamed et al. [14] has shown that the maximum temperature T_{max} is given by:

$$T_{max} = T_0 + 0.5A_0\left(0.5\rho^2 + \frac{\rho k}{Ha}\right), \tag{3.7}$$

where A_0 is such that:

$$A_0 = \frac{\sigma l_0 a^2}{k}\left(\frac{\rho_0}{\rho}\right)^2 exp(-2\sigma a N_0 n_0 \eta). \tag{3.8}$$

Equation (3.1) through (3.7) are generally known in W-shaped optical fiber analysis. Specifically, (3.8) is used in the analysis and regularization of the T_{max} for better communication transfer.

3.2.2 The Optimized Temperature Model (OWTOF)

In view of figure 3.3, denote by $f : \Re \to \Re$ a regularly varying function at infinity index of T such that:

$$f(T) = T^{v} L(T), \tag{3.9}$$

where v is an index of variation of T relative to any events and L is a slowly varying process on some neighborhood $[0, \infty)$ such that for an arbitrary $x \in \Re$, we have:

$$\lim_{T \to \infty} \frac{L(Tx)}{L(T)} = 1. \tag{3.10}$$

Given that $T = f(T)$ as claimed in figure 3.3, it implies that the known equations of the temperature for WTOF given below are equivalent equations with those represented at the right hand side:

$$\frac{1}{\rho}\frac{\partial}{\partial\rho}\left(\rho\frac{\partial T}{\partial\rho}\right) = -\frac{\sigma l_o a^2}{kF^2}\left(\frac{\rho_0}{\rho}\right)^2 exp(-2\sigma n_0 N_0 \eta - \frac{\rho^2}{F^2}) = \frac{1}{\rho}\frac{\partial}{\partial\rho}\left(\rho\frac{\partial f(T)}{\partial\rho}\right), \tag{3.11}$$

$$T_{max} = T_0 + 0.5 f(A_0)\left(0.5\rho^2 + \frac{\rho k}{Ha}\right) = f(T_0) + 0.5(A_0)\left(0.5\rho^2 + \frac{\rho k}{Ha}\right) = f(T_{max}), \tag{3.12}$$

$$A_0 = \frac{\sigma l_0 a^2}{k}\left(\frac{\rho_0}{\rho}\right)^2 exp(-2\sigma a N_0 n_0 \eta) = f(A_0), \tag{3.13}$$

$$l = \frac{k.F^2.(\log T)^2.ln10T^{\frac{1}{\rho}}}{\sigma a^2 \rho^3 exp\left(-2\sigma\sigma n N\eta - \frac{\rho^2}{F^2}\right)} = f(l) = \frac{k.F^2.(\log T)^2.ln10f(T^{\frac{1}{\rho}})}{\sigma a^2 \rho^3 exp\left(-2\sigma\sigma n N\eta - \frac{\rho^2}{F^2}\right)}. \tag{3.14}$$

W-shaped optical fiber designed under (3.9) and (3.10) as in (3.11), (3.12), (3.13) and (3.14) provide a regulation policy for T distinct from the one in (3.7) because of the optimized equations are in limiting distribution for each temperature affecting communication. Additionally, it can be envisaged that optimized equations as in (3.11), (3.12), (3.13) and (3.14) optimizes directly the W-shaped optical fiber in figure 3.1 by shifting temperature to its limits. Thus, solving delay and distortion problem as identified in section 1.6. Consequently, the optimized fiber in this sense if materialized is better suited for communication purposes than the existing non optimized ones because of the temperature control imposed in the design and analysis in view of (3.9) and (3.10). We incorporate (3.9) and (3.10) in the geometry of (3.6) to obtain limiting distribution for T as in (3.11), (3.12), (3.13) and (3.14) leading to an optimized version of (3.7) given that:

$$\frac{k}{a}\frac{\partial T}{\partial \rho}|_{\rho=\rho_0} = H\left(T_{max} - T_0\right). \tag{3.15}$$

3.2.3 Model Validation

For the purpose of validating the results of this work, the principle of content validation of Wiener [16] is applied. Specifically, the convergent type of content validity therein Wiener [16] is adopted to prove the convergence of the OWTOF design to that of WTOF model of Mohamed et al. [14] as in figure 3.1. The following proposition is made as a tool for validity of the optimized temperature model. In addition, the originality content of the entire work is tested using urkund software available in the library. Details of the plagiarism check is reported in appendix 1.

Proposition 3.2.1 *Given affecting parameters as specified in section (3.1), the optimized model is valid if there exists v and T in (3.9) such that:*

$$T^v L(T) = T_{max}, \tag{3.16}$$

where T_{max} is given by (3.7).

3.3 Objective 3: Performance Analysis

Results derived for the OWTOF presented in this work is compared analytically and via simulations with those of Mohamed et al. [14]. Specifically, the A_0, T_{max} and l are compared. The comparison is made in the light of all values of WTOF adopted for the WTOF in Mohamed et al. [14] for both WTOF and OWTOF. Also, stationary new values for uncommon parameters are constructed. Results on this comparison are carried out as discussions on the T_{max} behavior of the OWTOF model relative to WTOF. Additionally, numerical analysis for the l of the OWTOF relative to the WTOF is carried out. The designed MATLAB programs provide the base for performance comparison of the OWTOF with WTOF. Details of the MATLAB programs constructed for this purpose are given in appendix IV, appendix V, appendix VI, appendix VII, appendix $VIII$, appendix IX , appendix X and appendix XI.

3.4 Contribution to Knowledge

Two journal articles have been submitted. Details include

1. **Designing WTOF of Tomorrow**. Under review, IAENG Engineering Letters, 2018.

2. **WTOF Under Power Law Core Temperature Variation Condition**. Under review, IAENG International Journal of Applied Mathematics, 2018. See appendix II and appendix III for acknowledgments of the submitted articles.

Chapter 4

Results and Discussions

4.1 Research Question 1

What are the conditions for optimizing the maximum axial temperature of a WTOF?

Figure 3.2 and figure 3.3 provide basic strategy and optimization process for optimizing the temperature function in the core of WTOF in figure 3.1. From the former figures, it is clear that there are two conditions that are needed to optimize the T_{max} of the WTOF. First, ensuring that selected materials needed for designing the core of the WTOF are strong enough such that regularly varying temperature in the core cladding region are controlled via dominatedly non decreasing slowly varying function for regularly varying functions. Secondly, the design optimization process must ensure that the T_{max} distribution of the OWTOF coincides with that of the WTOF at a given point. Lemma 4.1.1 and lemma 4.1.2 provide detailed prove for the two optimizing conditions above.

Lemma 4.1.1 *The necessary condition for optimizing the T_{max} of a WTOF is the use of dominatedly non decreasing slowly varying function in the fiber design.*

Proof: Suppose $L(T)$ is chosen such that: $|L(Tx)| = |L(T) + L(x)|$; for all $x > 0$, we have by (3.10) that:

$$\lim_{T\to\infty}\frac{L(Tx)}{L(T)}=\lim_{T\to\infty}\frac{L(T)+L(x)}{L(T)}=1+\lim_{T\to\infty}\frac{L(x)}{L(T)}=1. \tag{4.1}$$

Additionally, in view of the definition of dominatedly non decreasing slowly varying function in Shimura [38], we have:

$$\lim_{T\to\infty} sup(L(Tx)-L(T))=\lim_{T\to\infty} sup(L(T)+L(x)-L(T))=L(x). \tag{4.2}$$

Hence L is realistic and suitable for regulating the temperature rising problem in WTOF.

Lemma 4.1.2 *if $q(T)$ is a slowly varying function suitable for optimizing WTOF as in lemma (4.1.1). Then, the following statements are equivalent.*

i. There exists a real valued function $r(T)$ that approximates $q(T)$.

ii. The limiting distribution of $r(T)$ coincide with that of $q(T)$.

Proof: To show that $i \implies ii$ under lemma (4.1.1), let $j(T)$ and $i(T)$ be any two arbitrary given positive functions. Then for any $x>0$, we have $j(Tx)>0$ and $i(Tx)>0$. Similarly, the ratio $\frac{j(Tx)}{j(T)}$ and $\frac{i(Tx)}{i(T)}$ are non negative. Denote by $q(T)$ and $r(T)$ the two preceding functions respectively. We see that as T grows large, the limit:

$$\lim_{T\to\infty}\left(\frac{\frac{i(Tx)}{i(T)}}{\frac{j(Tx)}{j(T)}}\right)=\frac{\lim_{T\to\infty}\frac{i(Tx)}{i(T)}}{\lim_{T\to\infty}\frac{j(Tx)}{j(T)}}=\lim_{T\to\infty}\frac{q(T)}{r(T)}>0, \tag{4.3}$$

if a unit convergent limit point is chosen for $q(T)$ and $r(T)$ then:

$$\lim_{T\to\infty}\frac{q(T)}{r(T)}=1>0, \tag{4.4}$$

holds. Thus, $i \implies ii$. Similarly, given that $q(T)$ coincides with $r(T)$ in distribution, then $q(T)$ approximate $r(T)$. So that $ii \implies i$.

4.2 Research Question 2

What analytic functions are suitable for designing an optimized WTOF strong enough to regularize the maximum temperature?
As in figure 3.3, since T_{max} changes with time depending on factors outside the domain of the fiber, materials for designing WTOF core must be dubbed enough to behave log-wise to effectively checked regularly varying temperature. Remark 4.2.1 and lemma 4.2.1 provide the required support for this answer. The lemmas show that if dubbing is effectively carried out on the core, temperature can be controlled to limiting value. This limiting temperature arising from effective dubbing of the core has any temperature within the limit. Thus, free from fuse effects, chromatic dispersion effects and rupture effects especially if the dobbing is in the light of radial position of the fiber core relative to the light source. Lemma 4.2.1 summarized this answer.

Remark 4.2.1 *A suitable function $L : |L(Tx)| \to |L(T)+L(x)|$ needed for the design of an optimized WTOF is a log-function. This is in view of lemma (4.1.1) above.*

Lemma 4.2.1 *The absolute temperature T of OWTOF under regularly varying assumption in (3.6) is given by:*

$$T = exp\left[\sqrt{\frac{\sigma l_o a^2}{kF^2}(\frac{\rho_0}{\rho})^2 ln10\rho^3 e^{\left(-2\eta\sigma N_0 n_0 - \frac{\rho^2}{F^2}\right)}}\right]^{\frac{\rho}{1+\rho}}. \tag{4.5}$$

Proof: Suppose $T = f(T)$ as claimed in the design of this OWTOF. Then in view of (3.9), one can write (3.6) as:

$$\frac{1}{\rho}\frac{\partial}{\partial\rho}\left(\rho\frac{\partial}{\partial\rho}T^v L(T)\right) = -\frac{\sigma l_o a^2}{kF^2}\left(\frac{\rho_0}{\rho}\right)^2 exp\left(-2\sigma n_0 N_0\eta - \frac{\rho^2}{F^2}\right). \tag{4.6}$$

Let $v = \frac{1}{\rho}$. Then in view of remark 4.1.1, one can write (4.6) as:

$$\frac{1}{\rho}\left(\frac{\partial}{\partial\rho}T^{\frac{1}{\rho}}\log T\right) = -\frac{\sigma l_o a^2}{kF^2}\left(\frac{\rho_0}{\rho}\right)^2 exp\left(-2\sigma n_0 N_0\eta - \frac{\rho^2}{F^2}\right). \tag{4.7}$$

Differentiating the left hand side of (4.7) partially with respect to ρ yields

$$T^{\left[\frac{1+\rho}{\rho}\right]} = exp\left[\sqrt{\frac{\sigma l_o a^2}{kF^2}(\frac{\rho_0}{\rho})^2 ln10\rho^3 e^{\left(-2\eta\sigma N_0 n_0 - \frac{\rho^2}{F^2}\right)}}\right] \tag{4.8}$$

The lemma follows by taking the unit of both indices in (4.8) above, one can obtain (4.5).

4.3 Research Question 3

How can the OWTOF behaved in performance relative to the WTOF? Suppose a WTOF in figure 3.1 is designed under figure 3.2 and processed under figure 3.3. By lemma 4.1.1, the temperature variation is dominatedly non decreasing and slowly varying given values of affecting parameters. Under this condition, the fiber (OWTOF) regulates any temperature rise better than the WTOF since $logT < T$. Thus, in terms of temperature control, the OWTOF is a better fiber than the WTOF even though the two fiber coincides with each other after some times; lemma 4.1.2. Additionally, the OWTOF scales temperature variations more better than the WTOF. This is in view of table 4.1, table 4.2 and table 4.3 showing that the OWTOF has high resistivity as manifested in the high values of the A_0 relative to heat scaling; see also appendix XII, appendix XIII and appendix XIV. In terms of cooling ability, the OWTOF can perform better than the WTOF. This is in view of appendix XV, appendix XVI and appendix XVII showing that at various sizes of the T, the OWTOF cools faster than the WTOF. Hence, the OWTOF is expected to perform better than the WTOF in terms of controlling the fuse effects and rupture effects; see also table 4.4, table 4.5 and table 4.6 for changes in ρ of the two fibers. Lemma 4.3.1, lemma 4.3.2 and lemma 4.3.3 summarized the performance advantage of the OWTOF over the WTOF.

Lemma 4.3.1 *The normalized T_{max} for the OWTOF fiber designed in this work is given by:*

$$T_{max} = T_0 + \frac{k}{Ha\rho^2 \ln 10}(\ln TT^{\frac{1}{2\rho}})^2. \tag{4.9}$$

Proof: In view of (3.9), one can write (3.15) as:

$$\frac{k}{a}\frac{\partial T^v L(T)}{\partial \rho}|_{\rho=\rho_0} = H(T_{max} - T_0). \tag{4.10}$$

Put $v = \frac{1}{\rho}$, where $L(T)$ is a log-function. Then:

$$\frac{k}{a}\frac{\partial T^{\frac{1}{\rho}} \log T}{\partial \rho}|_{\rho=\rho_0} = H(T_{max} - T_0). \tag{4.11}$$

Upon differentiating the left hand side of (4.11) with respect to ρ yields:

$$-\frac{k}{a\rho^2 \ln 10}(\ln TT^{\frac{1}{2\rho}})^2 = H(T_{max} - T_0). \tag{4.12}$$

Let H^{-1} denote the inverse of convection heat transfer coefficient H. We have:

$$-\frac{k}{aH\rho^2 \ln 10}(\ln TT^{\frac{1}{2\rho}})^2 = T_{max} - T_0. \tag{4.13}$$

Finally, the lemma follows upon transferring T_0 to the left hand side of (4.13) and normalizing the said equation.

Lemma 4.3.2 *The A_0 for the OWTOF is given by:*

$$A_0 = \frac{1}{2}\frac{k}{\rho^2}\log T. \tag{4.14}$$

Proof: Rearranging the second component on the right hand side of (4.9), one obtains that:

$$T_{max} = T_0 + \frac{k}{Ha\rho^2 \ln 10}\left(\ln T + \ln T^{\frac{1}{2\rho}}\right)^2. \tag{4.15}$$

Upon simplifying (4.15) yields:

$$T_{max} = T_0 + \frac{1}{4}\frac{k}{\rho^2}\log T\left(\ln T\left(\frac{4\rho^2 + 4\rho + 1}{aH\rho^2}\right)\right). \tag{4.16}$$

The lemma follows by comparing (4.16) with (3.7) for A_0 and rearrangement.

Lemma 4.3.3 *The intensity of light passed on the OWTOF is given:*

$$l = \frac{k.F^2.\log(T)^2.ln10T^{\frac{1}{\rho}}}{\sigma a^2\rho^3 exp\left(-2\sigma\sigma nN\eta - \frac{\rho^2}{F^2}\right)}. \tag{4.17}$$

Proof: In view of (3.9), one can write (3.6) as:

$$\frac{1}{\rho}\left(\frac{\partial}{\partial\rho}T^v L(T)\right) = -\frac{\sigma l_o a^2}{kF^2}\left(\frac{\rho_0}{\rho}\right)^2 exp(-2\sigma n_0 N_0\eta - \frac{\rho^2}{F^2}), \tag{4.18}$$

where $v = \frac{1}{\rho}$ and $L(T)$ is log-function. Then:

$$\frac{1}{\rho}\left(\frac{\partial}{\partial\rho}T^{\left(\frac{1}{\rho}\right)}\log T\right) = \frac{\sigma l_o a^2}{kF^2}\left(\frac{\rho_0}{\rho}\right)^2 exp(-2\sigma n_0 N_0\eta - \frac{\rho^2}{F^2}). \tag{4.19}$$

Upon differentiating the left hand side of (4.19) one can obtained:

$$\frac{1}{\rho^3}\log T.lnT.T^{\left(\frac{1}{\rho}\right)} = \frac{\sigma l_o a^2}{kF^2}\left(\frac{\rho_0}{\rho}\right)^2 exp(-2\sigma n_0 N_0\eta - \frac{\rho^2}{F^2}). \tag{4.20}$$

The lemma follows upon transferring l_0 to the left hand side of (4.20) to obtain:

$$l_0 = \frac{k.F^2.\log(T)^2.ln10T^{\frac{1}{\rho}}}{\sigma a^2.\rho^3 exp\left(-2\sigma\sigma n_0 N_0\eta - \frac{\rho^2}{F^2}\right)}, \tag{4.21}$$

and taking away subscriptions on both sides of (4.21).

4.4 Numerical Simulations and Validation

For numerical simulations and validation of the OWTOF fiber designed in this work, Mohamed et al. [14] values are adopted for the WTOF and OWTOF designed in this work. For these adopted values, the behavior of the A_0 (WTOF) and A_0 (OWTOF) are numerically simulated and compared. Additionally, the T_{max} (WTOF) and T_{max} (OWTOF) are simulated as functions of the radial position ρ and compared. The following numerical values and simulations are obtained.

Remark 4.4.1 *The scale constant A_o for the OWTOF designed in this work converges to that of WTOF.*

Table 4.1,table 4.2 and table 4.3 provide summary of the relationship between the OWTOF and the WTOF in terms of A_0 for selected values of ρ. It can be seen that the A_0 values for OWTOF are decreasing faster to zero, more faster than the decreasing rate for WTOF (see also appendix XII, appendix XIII and appendix XIV). That clearly implies the existence of a unique value for ρ when the A_0 of the two fibers coincides with each other. Consequently, the OWTOF designed in this work is valid. This can be seen in table 4.1, table 4.2 and table 4.3 above that when ρ values range between (0.1 - 2.0), the constant remaining temperature A_0 for the OWTOF converges fast to zero similar to that of the WTOF. Interestingly, the OWTOF fiber designed in this work start with A_0 significantly higher than that of WTOF. It can be concluded the OWTOF is an upgrade of WTOF. Similar result and relationship could be rerad from appendix XII, appendix XIII and appendix XIV below.

Remark 4.4.2 *The maximum temperature T_{max} for the OWTOF designed in this work converges absolutely with that of the WTOF.*

This is clearly seen from the table 4.4, table 4.5 and table 4.6. One can see that the T_{max} corresponding to the OWTOF designed in this work decreases faster for ρ values in the neighborhood of (0.1, 2.0). Additionally, the similarity between the OWTOF and the WTOF in terms of T_{max} becomes more glaring as $\rho \to 2.0$ (see also appendix XV, appendix XVI and appendix XVII). Interestingly, the distributions of the two fibers coincide absolutely at $\rho = 2.0$ (see also appendix XV and appendix XVI). The implication here is that, it is possible to construct a fiber whose initial T_{max} is higher than expected and can be made to behave absolutely like the existing WTOF. The absolute convergence of T_{max} for OWTOF to that of WTOF means that the problem of unnecessary distortion and delays in communication due to rise in temperature can be solved by the OWTOF designed in this work if realized. This is in view of the fast convergence rate of OWTOF to that of the WTOF and its absolute nature.

Table-4.1: $\mathbf{A}_0$ against ρ at $T = 1.2$

ρ	A_0 WTOF	A_0 OWTOF
0.1000	0.0420100	10.6700000
0.2000	0.0105000	2.6660000
0.4000	0.0026260	0.6666000
0.6000	0.0011670	0.2963000
0.8000	0.0006564	0.1667000
1.0000	0.0004201	0.1067000
1.1000	0.0003472	0.0881500
1.4000	0.0002143	0.0544200
1.8000	0.0001297	0.0329200
2.0000	0.0001050	0.0266600

4.5 Fiber Effects in OWTOF and WTOF

In this section, simulation analysis of the fuse effect, rupture effect and chromatic dispersion effect on the OWTOF and the WTOF are carried out. To estimate the fuse effect, we suppose that a laser beam of light is passed onto both fibers at a given temperature under varied propagation distance η. The l as a unit of stored energy for various η was simulated and compared. Define the fuse effect in both fibers as:

$$fuse\ effect \ = \ \frac{l}{\eta}. \tag{4.22}$$

Under (4.23), we posit that a fiber is better if the fuse effect tendency is lower than that of another fiber; Junior et al. [1]. Additionally, let the rupture effect be defined as:

$$rupture\ effect \ = \ \frac{l_{extreme}}{\eta}. \tag{4.23}$$

Finally, we defined the chromatic dispersion; Junior et al. [1] as:

$$chromatic\ dispersion \ = \ \frac{l_{extreme}}{\eta} - \frac{l}{\eta}. \tag{4.24}$$

Table-4.2: A_0 against ρ at $T = 1.5$

ρ	A_0 WTOF	A_0 OWTOF
0.1000	0.0420100	23.72000
0.2000	0.0105000	5.930000
0.4000	0.0026260	1.482000
0.6000	0.0011670	0.658900
0.8000	0.0006564	0.370600
1.0000	0.0004201	0.237200
1.1000	0.0003472	0.196000
1.4000	0.0002143	0.121000
1.8000	0.0001297	0.073210
2.0000	0.0001050	0.059300

Table-4.3: $\mathbf{A}_0$ against ρ at $T = 1.7$

ρ	A_0 WTOF	A_0 OWTOF
0.1000	0.0420100	31.0400000
0.2000	0.0105000	7.7600000
0.4000	0.0026260	0.4000000
0.6000	0.0011670	0.8623000
0.8000	0.0006564	0.4850000
1.0000	0.0004201	0.3104000
1.1000	0.0003472	0.2565000
1.4000	0.0002143	0.1584000
1.8000	0.0001297	0.0958100
2.0000	0.0001050	0.0776000

Table-4.4: T_{max} against ρ at $T = 1.3$

ρ	T_{max} WTOF	T_{max} OWTOF
0.2000	20.06000	23.52000
0.4000	20.03000	20.52000
0.6000	20.02000	20.21000
0.8000	20.02000	20.10000
1.0000	20.01000	20.06000
1.2000	20.01000	20.04000
1.4000	20.01000	20.03000
1.6000	20.01000	20.02000
1.8000	20.01000	20.02000
2.0000	20.01000	20.01000

Table-4.5: T_{max} against ρ at $T = 1.5$

ρ	T_{max} WTOF	T_{max} OWTOF
0.2000	20.06000	23.65000
0.4000	20.03000	20.59000
0.6000	20.02000	20.21000
0.8000	20.02000	20.11000
1.0000	20.01000	20.06000
1.2000	20.01000	20.04000
1.4000	20.01000	20.03000
1.6000	20.01000	20.02000
1.8000	20.01000	20.02000
2.0000	20.01000	20.01000

Table-4.6: T_{max} against ρ at $T = 1.6$

ρ	T_{max} WTOF	T_{max} OWTOF
0.2000	20.06000	24.91000
0.4000	20.03000	20.79000
0.6000	20.02000	20.29000
0.8000	20.02000	20.14000
1.0000	20.01000	20.08000
1.2000	20.01000	20.06000
1.4000	20.01000	20.04000
1.6000	20.01000	20.03000
1.8000	20.01000	20.02000
2.0000	20.01000	20.02000

Equations (4.22), (4.23) and (4.24) are used to answer research questions 4, 5 and 6 below.

4.6 Research Question 4

Suppose a telecommunication service user sends a message when the core of the fiber experiences a temperature rise. What is the expected fuse effects on WTOF and optimized WTOF?

Appendix XVIII and appendix XIX summarized the relationship between l and η. Suppose a telecommunication service user sends a message to a receiver one unit of distant apart when the temperature of the core rises. By (4.22), the energy of WTOF is 1464000 units and the energy of OWTOF is 1365000 units. In this case, the WTOF stored more energy than the OWTOF. In this case, the temperature rise tendency that may lead to the fuse effect is higher in the WTOF than the OWTOF. Similar fuse effect are experienced for lower η to the advantage of OWTOF (see also table

4.7 and table 4.8). There is a need to optimize the OWTOF in the light of another parameter. This is sequel to the behavior of OWTOF after one unit of η.

4.7 Research Question 5

Suppose a telecommunication service user sends a message when the core of the fiber experiences a temperature rise. What is the expected rupture effects on WTOF and optimized WTOF?

Table 4.7 and table 4.8 summarized the relationship between l and η. From this figures if η is less than one unit of propagation, the WTOF is more liable to experience the rupture effect especially if the energy gradient for smooth communication is far below 99000 units. Within this distance, if a service user sends a message, the core of the WTOF experiences more temperature rise than that of the OWTOF. This is in view of the excess energy of 99000 units as variation energy between the WTOF and the OWTOF (See also appendix XVIII and appendix XIX).

4.8 Research Question 6

Suppose a telecommunication service user sends a message when the core of the fiber experiences a temperature rise. What is the expected chromatic dispersion effects on WTOF and optimized WTOF?

Appendix XVIII and appendix XIX summarized the relationship between l and η. From this figures, it can be see that if η is less than one unit of propagation, the WTOF core is more liable to experience high chromatic dispersion effect especially if the stored energy is far below 99000 units than the OWTOF. The excess 99000 units of energy are more likely to concentrate around the core cladding region of the WTOF causing chromatic distortion problems in communication. This is evidenced that below 99000 units the variation energy is higher than that of the OWTOF (See

Table-4.7: l against η at $T = 1.02$

η	l WTOF (10^{06})	l OWTOF (10^{06})
0.200	1.4630	0.9909
0.400	1.4630	1.0730
0.600	1.4630	1.1630
0.800	1.4630	1.2600
1.000	1.4640	1.3650
1.175	1.4640	1.4640
1.176	1.4640	1.4640
1.200	1.4640	1.4780
1.800	1.4650	1.8790
2.000	1.4650	2.0360

also table 4.7 and table 4.8).

Table-4.8: l **against** η **at** $T = 1.04$

η	l WTOF (10^{06})	l OWTOF (10^{06})
0.200	1.4630	0.9217
0.400	1.4630	0.9984
0.600	1.4630	1.0820
0.800	1.4630	1.1720
1.000	1.4640	1.2690
1.200	1.4640	1.3750
1.356	1.4640	1.4640
1.357	1.4640	1.4640
1.800	1.4650	1.7480
2.000	1.4650	1.8940

Chapter 5

Recommendations and Conclusion

5.1 Summary of the Work

This research work designs an optimized WTOF. The aim is to create a WTOF that can resist the effect of temperature rise in W-shaped core refractive index optical fiber for better communication. Using the concept of regularly varying function, we provide a functional fiber whose resistance to temperature variations surpasses that of WTOF. Additionally, the A_0 for OWTOF designed in this work is shown to converge absolutely with that of the WTOF. This implies that the OWTOF can transcend over the WTOF in term of scaling temperature without causing any thermal effect. Finally, the research work achieves the three objectives specified in chapter one via both the analytical and numerical results proved in chapter four of this work.

5.2 Recommendations

For the purposes of improving this work, the following recommendations are drawn

5.2.1 Recommendation Arising from Objective 1

In objective 1, the formulation of three stage optimization strategy that can minimize temperature rise in the core of WTOF is stated. This objective is presented in figure 3.2 and figure 3.3. Essentially, the strategy involves describing the transient temperature in existing WTOF as a limiting temperature whose changes is regularly varying at infinity index of the ρ. This objective is achieved in lemma 4.1.1 and lemma 4.1.2. Unfortunately, when the l is plotted against the η (see also appendix XVIII and appendix XIX), the designed OWTOF shows improvement on the WTOF only at η around one unit of distance. But fibers are generally known to be propagated over long distances more than one unit. This suggests the need for a higher optimization strategy that will make the OWTOF better than the WTOF even at longer propagation distances. In this regard, a four stage optimization strategy involving an extension of the optimal space of figure 3.2 to a buffer space involving advanced temperature control functions is recommended to further this research work. It is believed that such functions may regulate further the intensity of light over long propagation distances without fear of thermal effects studied in this work.

5.2.2 Recommendation Arising from Objective 2

In objective 2, the design of functional temperature models under the three stage optimization strategy formulated in figure 3.2 and figure 3.3 that regulates temperature rise in WTOF are stated. Three temperature models lemma 4.2.1, lemma 4.3.1 and lemma 4.3.2 are designed and proved under figure 3.2 and figure 3.3. As identified in literature gap number 2, the models precedes the fiber and are better (remark 4.2.1 and remark 4.2.2) than the existing models in regulating the temperature rise causing distortion and delay problems in communication studied in this work. The work recommends the construction of the OWTOF as a means of mitigating thermal effects harmful to better communication.

5.2.3 Recommendation Arising from Objective 3

In objective 3, the test of the three temperature functional models under the three stage optimization strategy designed in figure 3.2 and figure 3 is stated. The test is carried out via numerical simulation of models versus affecting parameters (see also appendix XII, appendix XIII and appendix XIV, appendix XV, appendix XVI and appendix XVII). Additionally, (see also appendix XVIII and appendix XIX). The comparisons are carried out by comparing the OWTOF and the WTOF under the same conditions (see also remark 4.2.1, remark 4.2.2, table 4.7 and table 4.8). The comparisons are carried out under few cases of the affecting parameters due to time and space namely; intensity of light passed on the fiber core, the radial position and the propagation distance. There is need to test the models derived in this work against other parameters such as index tailoring parameters etc for a better fiber.

5.3 Conclusion

This research work provides a three stage optimization strategy for regulating the effects of temperature rise in WTOF (figure 3.2). The strategy is applied on WTOF (figure 3.3) and analysis leading to new temperature models over regularly varying temperature conditions are carried out (equations 4.9, 4.14 and 4.17). Six research questions (section 1.9) on optimizing the WTOF are answered (sections 4.1, 4.2, 4.3, 4.6, 4.7 and 4.8). The work shows that the necessary condition for designing an OWTOF that regularizes rise in T_{max} is the use of dominatedly non decreasing slowly varying function in the fiber design (lemma 4.1.1). In addition the distribution of the OWTOF and the WTOF must coincide for validation (lemma 4.1.2). Furthermore, numerical simulations and comparisons were carried out and results stated (see also table 4.1, table 4.2, table 4.3, table 4.4, table 4.5, table 4.6, table 4.7 and table 4.8) and proved leading to the OWTOF. Also, remarks (remarks 4.2.1, 4.4.1 and 4.4.2) covering the performance of the OWTOF in relation to the WTOF are stated and explained. The designed OWTOF presented in this work checks the effect of rising temperatures for better communication (appendix XII, appendix XIII and appendix XIV, appendix XV, appendix XVI and appendix XVII, appendix XVIII and appendix XIX). This is in view of results generated in this work. Finally, three recommendations for furthering this research are given (section 5.2).

Appendices

Appendix-I

Dhdr Inquiries <dhdrinquiries@kiu.ac.ug>

6:30 AM (10 hours ago)

to me

---------- Forwarded message ----------

From: <report@analysis.urkund.com>

Date: Tue, Aug 14, 2018 at 4:27 PM

Subject: [Urkund] 1% similarity - kyevugas@gmail.com

To: dhdrinquiries@kiu.ac.ug

Document sent by: kyevugas@gmail.com

Document received: 8/14/2018 3:26:00 PM

Report generated 8/14/2018 3:27:24 PM by Urkund's system for automatic control.

Student message: Good afternoon sir, am kyevuga simon peter,

REG NO. 1163-03216-08406 a master student taking a master degree

in electrical engineering. Am humbly requesting for testing my thesis

for plagiarism as soon as possible and i will attach the test result

together with the entire work and resend it to the external examiner.

i will be grateful if my request is considered

positively. Thanks

Document : SIMON THESIS.pdf [D40817731]

About 1% of this document consists of text similar to text found in 54 sources.

The largest marking is 18 words long and is 100% similar to its primary source.

PLEASE NOTE that the above figures do not automatically mean that

there is plagiarism in the document. There may be good reasons as to

why parts of a text also appear in other sources. For a reasonable

suspicion of academic dishonesty to present itself, the analysis, possibly found

sources and the original document need to be examined closely. Click here to

open the analysis:

https://secure.urkund.com/view/39964606-726799-858918

Click here to download the document:

https://secure.urkund.com/archive/download/40817731-962622-533545

Appendix-II

Acknowledgment of manuscript submission for the journal

Engineering Letters

Inbox x

IAENG Journal - EL <el@iaeng.org>

Jul 9

to me

Dear Sir/Madam,

~~ Acknowledgment of manuscript submission for the journal Engineering Letters ~~

Thank you for your manuscript submission. The manuscript has been assigned

manuscript number, EL_2018_06_29a, of title [Designing WTOF of Tomorrow].

You need to check the publication ethics and publication malpractice statement

available at http://www.engineeringletters.com/doc/publication_ethics.html

The average review time is three months. Suppose you has not got the review result by three months after getting the acknowledgement email, you are welcome to make the paper status enquiry with the manuscript number, EL_2018_06_29a.

The manuscript will be sent to our reviewer in the related field. During the reviewing process, if the reviewer decides that the manuscript should be accepted with major revision or rejected, we will usually arrange another reviewer for reviewing the manuscript to check if the reviewing results are consistent.

We will contact you again once we have received the reviews. The average acceptance rate of the regular research papers in our journal is less than 10%.

This reviewing process is to ensure the quality of the accepted papers in our journal, and we are looking forward to your understanding.

If you have any question, you are welcome to tell us.

Best regards,

Joan Mok

Assistant Secretary

Engineering Letters

Email: el@iaeng.org

www.engineeringletters.com

IAENG Secretarial

International Association of Engineers

Unit 1, 1/F, 37-39 Hung To Road, Hong Kong

IAENG Conferences:

Appendix-III

Acknowledgment of manuscript submission for the IAENG

International Journal of Applied Mathematics

Inbox x

IAENG Journal - IJAM <ijam@iaeng.org>

Aug 3 (6 days ago)

to me

Dear Sir/Madam,

~~ Acknowledgment of manuscript submission for the IAENG International Journal of Applied Mathematics ~~

Thank you for your manuscript submission. The manuscript has been assigned manuscript number, IJAM_2018_07_23c, of title [WTOF Under Power Law Core Temperature Variation Condition].

You need to check the publication ethics and publication malpractice statement available at http://www.iaeng.org/IJAM/doc/publication_ethics.html

The average review time is three months. Suppose you has not got the review result by three months after getting the acknowledgement email, you are welcome to make the paper status enquiry with the manuscript number, IJAM_2018_07_23c.

The manuscript will be sent to our reviewer in the related field. During the reviewing process, if the reviewer decides that the manuscript should be accepted with major revision or rejected, we will usually arrange another reviewer for reviewing the manuscript to check if the reviewing results are consistent.

We will contact you again once we have received the reviews.

The average acceptance rate of the regular research papers of our IAENG journals is less than 10%. This reviewing process is to ensure the quality of the accepted papers in our journal, and we are looking forward to your understanding.

If you have any question, you are welcome to tell us.

Best regards,

Joan Mok

Assistant Secretary

IAENG International Journal of Applied Mathematics

Email: ijam@iaeng.org

http://www.iaeng.org/IJAM

IAENG Secretarial

International Association of Engineers

Unit 1, 1/F, 37-39 Hung To Road, Hong Kong

IAENG Conferences:

Appendix-IV

```
 {\bf{MATLAB CODES THAT GENERATE A_{0}}} \\
clear; clc;
k = 1.17; Io = 10^10; a = 2*10^-3; rho_o = 0.1; sigma = 0.2;
eta = 10000; No = 1; T = 1.2; no = 1.5;
rho = [0.1:0.1:2];
Ao_mohammed = sigma*Io*a^2/k*(rho_o./rho).^2*exp(-2*sigma*a*eta*No*no);
Ao_peter = 0.5*k./rho.^2*log(T);
subplot(1,2,1), plot(rho, Ao_mohammed, 'b')
xlabel('rho')
ylabel('Ao')
title('Ao against rho: (WTOF)')
grid on
hold on
subplot(1,2,2), plot(rho, Ao_peter, 'r')
xlabel('rho')
ylabel('Ao')
title('Ao  against rho: (OWTOF)' )
```

```
grid on
```

Appendix-V

```
 {\bf{MATLAB CODES THAT GENERATE A_{0}}} \\
clear;\\
clc;\\
To = 20; k = 1.17; Io = 10^10; a = 2*10^-3; rho_o = 0.1; sigma = 0.2;\\
eta = 10000; No = 1; T = 1.5; no = 1.5;\\
rho = [0.1:0.1:2];\\
Ao_WTOF= sigma*Io*a^2/k*(rho_o./rho).^2*exp(-2*sigma*a*eta*No*no);\\
Ao_OWTOF = 0.5*k./rho.^2*log(T);\\
subplot(1,2,1), plot(rho, Ao_WTOF,)\\
xlabel('rho')\\
ylabel('Ao')\\
title('Ao against rho: (WTOF)')\\
grid on\\
hold on\\
subplot(1,2,2), plot(rho, Ao_OWTOF)\\
xlabel('rho')\\
ylabel('Ao')\\
title('Ao  against rho: (OWTOF)' )\\
grid on
```

Appendix-VI

```
 {\bf{MATLAB CODES THAT GENERATE A_{0}}} \\
clear; clc;
```

```
k = 1.17; Io = 10^10; a = 2*10^-3; rho_o = 0.1; sigma = 0.2;
eta = 10000; No = 1; T = 1.7; no = 1.5;
rho = [0.1:0.1:2];
Ao_mohammed = sigma*Io*a^2/k*(rho_o./rho).^2*exp(-2*sigma*a*eta*No*no);
Ao_peter = 0.5*k./rho.^2*log(T);
subplot(1,2,1), plot(rho, Ao_mohammed, 'b')
xlabel('rho')
ylabel('Ao')
title('Ao against rho: (WTOF)')
grid on
hold on
subplot(1,2,2), plot(rho, Ao_peter, 'r')
xlabel('rho')
ylabel('Ao')
title('Ao  against rho: (OWTOF)' )
grid on
```

Appendix-VII

```
{\bf{MATLAB CODES THAT GENERATE T_{max}}} \\
clear;\\
clc;\\
To = 20; k = 1.17; Io = 10^10; a = 2*10^-3; rho_o = 0.1; sigma = 0.2;\\
eta = 10000; No = 1; T = 1.3; no = 1.5; H = 10;\\
rho = [0.1:0.001:2];\\
Ao_WTOF = sigma*Io*a^2.*(rho_o./rho).^2.*exp(-2*sigma*a.*eta*No*no)/k;\\
Ao_OWTOF = 0.5*k./rho.^2*log(T);\\
Tmax_OWTOF = To + Ao_OWTOF.*log(T*(T.^(1./(2.*rho))));\\
```

```
Tmax_WTOF = To + 0.5*Ao_WTOF.*(0.5*rho.^2 + k.*rho./(H*a));\\
subplot(1,2,1), plot(rho, Tmax_WTOF,)\\
xlabel('rho')\\
ylabel('Tmax')\\
title('Tmax against rho (WTOF)')\\
grid on\\
hold on\\
subplot(1,2,2), plot(rho, Tmax_OWTOF,)\\
xlabel('rho')\\
ylabel('Tmax')\\
%zoom on
title('Tmax  against rho (OWTOF)')\\
grid on
```

Appendix-VIII

```
{\bf{MATLAB CODES THAT GENERATE T_{max}}} \\
clear; clc;
To = 20; k = 1.17; Io = 10^10; a = 2*10^-3; rho_o = 0.1; sigma = 0.2;
eta = 10000; No = 1; T = 1.5; no = 1.5; H = 10;
rho = [0.1:0.001:2];
Ao_mohammed = sigma*Io*a^2.*(rho_o./rho).^2.*exp(-2*sigma*a.*eta*No*no)/k;
Ao_peter = 0.5*k./rho.^2*log(T);
Tmax_peter = To + Ao_peter.*log(T*(T.^(1./(2.*rho))));
Tmax_mohammed = To + 0.5*Ao_mohammed.*(0.5*rho.^2 + k.*rho./(H*a));
subplot(1,2,1), plot(rho, Tmax_mohammed, 'b')
xlabel('rho')
ylabel('Tmax')
```

```
title('T_{max} against rho - Mohammed()')
grid on
hold on
subplot(1,2,2), plot(rho, Tmax_peter, 'r')
xlabel('rho')
ylabel('Tmax')
%zoom on
title('T_{max}  against rho')
grid on
```

Appendix-IX

```
{\bf{MATLAB CODES THAT GENERATE T_{max}}} \\
clear; clc;
To = 20; k = 1.17; Io = 10^10; a = 2*10^-3; rho_o = 0.1; sigma = 0.2;
eta = 10000; No = 1; T = 1.6; no = 1.5; H = 10;
rho = [0.1:0.01:2];
Ao_mohammed = sigma*Io*a^2.*(rho_o./rho).^2.*exp(-2*sigma*a.*eta*No*no)/k;
Ao_peter = 0.5*k./rho.^2*log10(T);
Tmax_peter = To + Ao_peter.*log(T*(T.^(1./(2.*rho))));
Tmax_mohammed = To + 0.5*Ao_mohammed.*(0.5*rho.^2 + k.*rho./(H*a));
subplot(1,2,1), plot(rho, Tmax_mohammed, 'b')
xlabel('rho')
ylabel('Tmax')
title('T_{max} against rho - Mohammed()')
grid on
hold on
subplot(1,2,2), plot(rho, Tmax_peter, 'r')
```

```
xlabel('rho')
ylabel('Tmax')
%zoom on
title('T_{max}  against rho')
grid on
```

Appendix-X

```
{\bf{MATLAB CODES THAT GENERATE $l$}} \\
clear; clc;
rho = 0.6; A = 1; a = 2*10^-3; sigma = 0.2; N = 1; T = 1.02;
n = 1; F = 1; k = 1.17;
eta = [0.1:0.001:2];
l_mohammed = A*k./(sigma*a^2*exp(-2*sigma*a*N*n*eta));
p_simon = k*F^2*log(T^2)*log(10)*T^(1./rho)./(rho^3*sigma*a^2*exp(-(2*sigma*N*n*eta) -
(rho^2/F^2)));
subplot(1,2,1), plot(eta, l_mohammed, 'b')
xlabel('eta')
ylabel('l')
title('l against eta (WTOF)')
grid on
hold on
subplot(1,2,2), plot(eta, p_simon, 'r')
xlabel('eta')
ylabel('l')
%zoom on
title('l against eta (OWTOF)')
grid on
```

Appendix-XI

```
{\bf{MATLAB CODES THAT GENERATE $l$}} \\
clear; clc;
rho = 0.9; A = 1; a = 2*10^-3; sigma = 0.2; N = 1; T = 1.04;
n = 1; F = 1; k = 1.17;
eta = [0.1:0.001:2];
l_mohammed = A*k./(sigma*a^2*exp(-2*sigma*a*N*n*eta));
p_simon = k*F^2*log(T^2)*log(10)*T^(1./rho)./(rho^3*sigma*a^2*exp(-(2*sigma*N*n*eta) -
(rho^2/F^2)));
subplot(1,2,1), plot(eta, l_mohammed, 'b')
xlabel('eta')
ylabel('l')
title('l against eta (WTOF)')
grid on
hold on
subplot(1,2,2), plot(eta, p_simon, 'r')
xlabel('eta')
ylabel('l')
%zoom on
title('l against eta (OWTOF)')
grid on
```

Appendix-XII

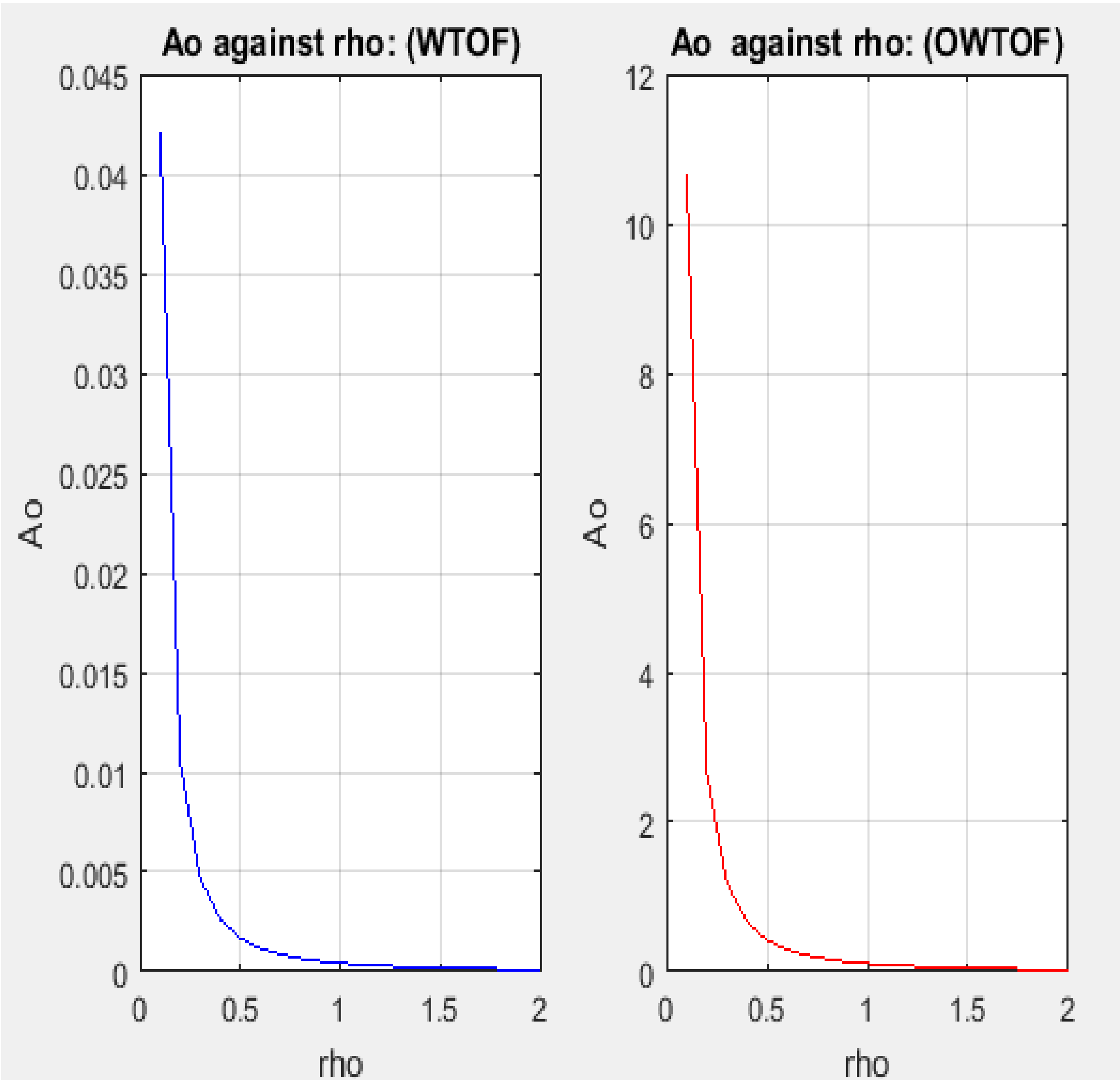

Figure 5.1: Variation of A_0 with ρ at $T = 1.2$

Appendix-XIII

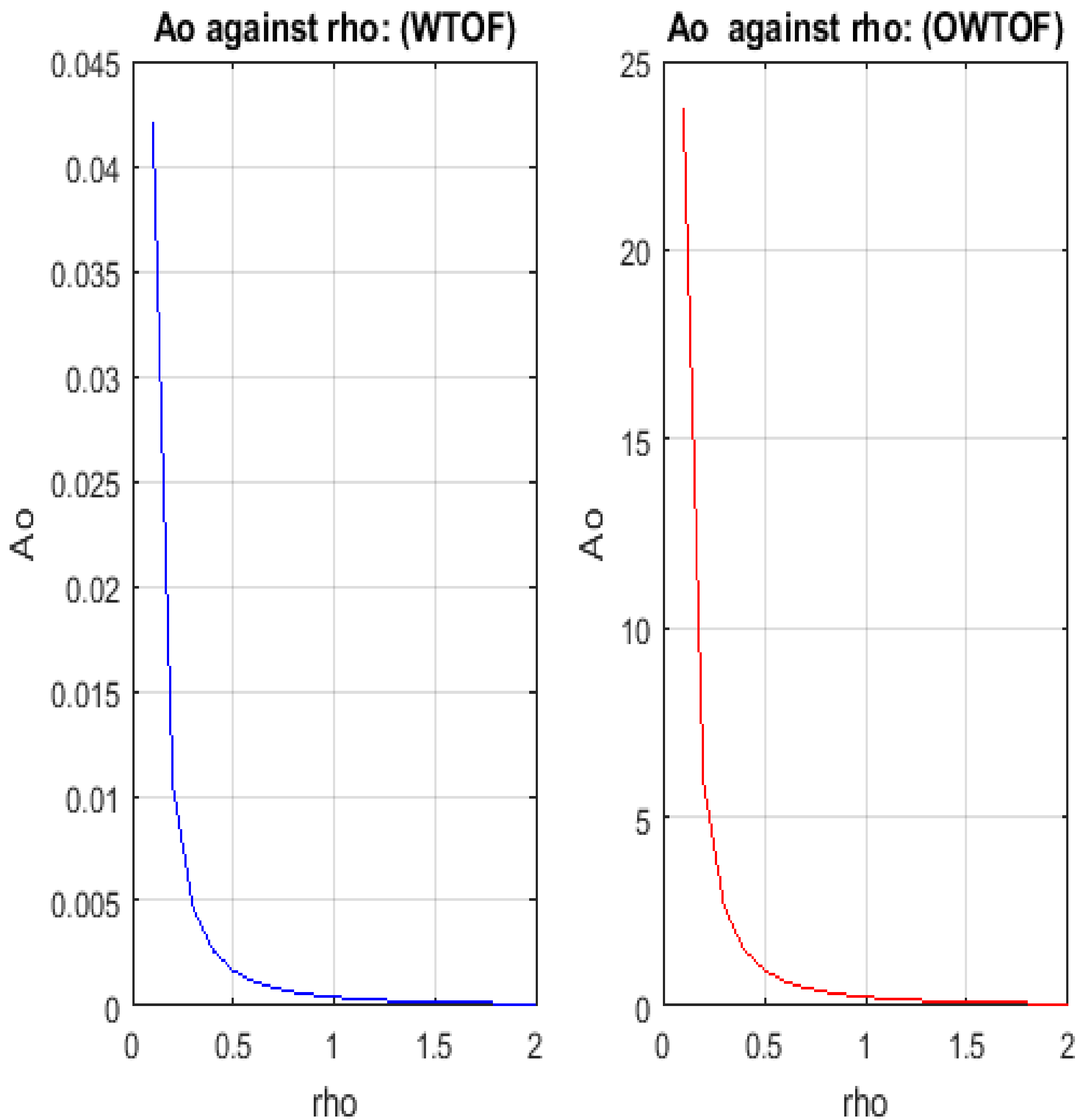

Figure 5.2: Variation of A_0 with ρ at $T = 1.5$

Appendix-XIV

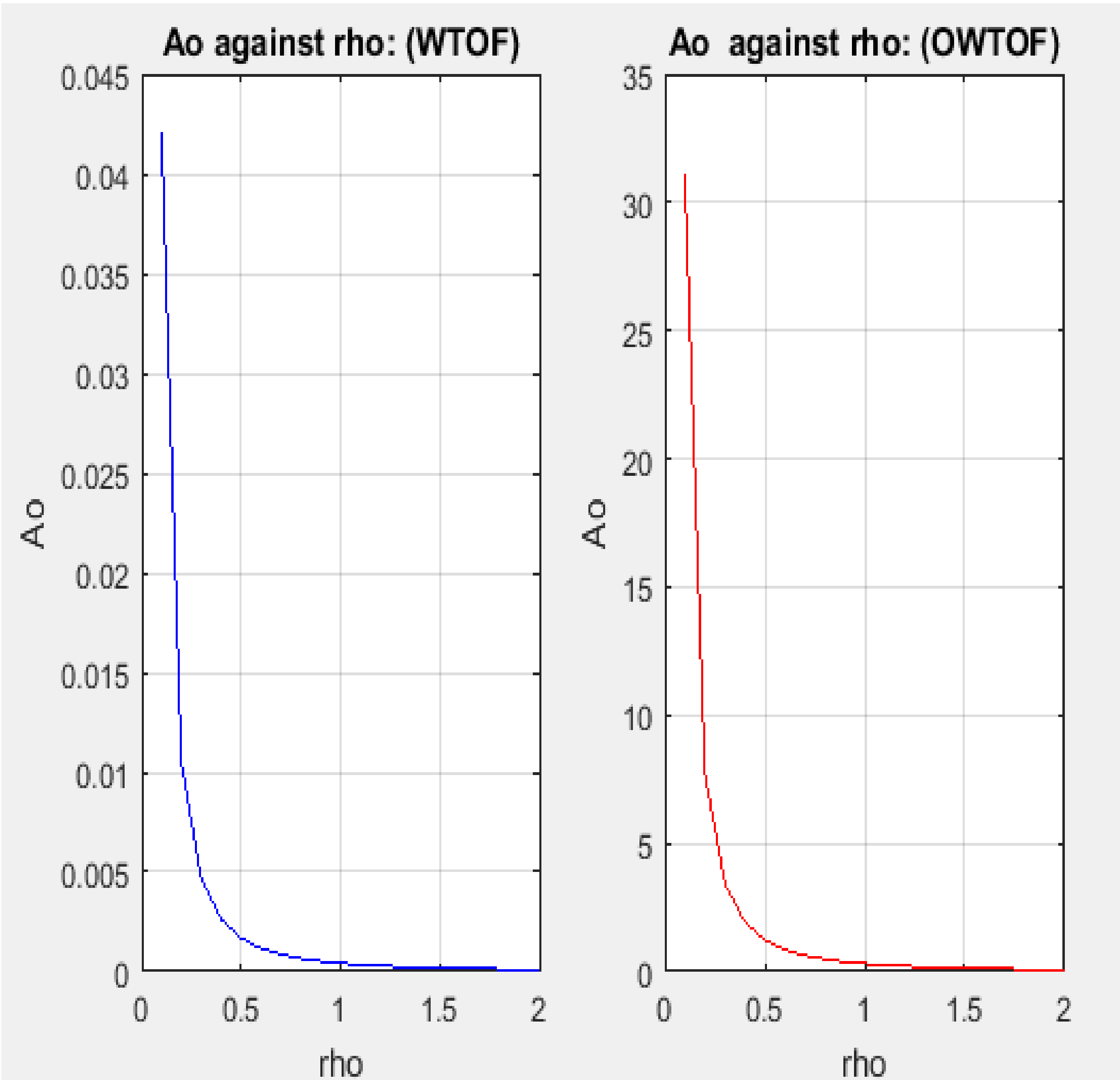

Figure 5.3: Variation of A_0 with ρ at $T = 1.7$

Appendix-XV

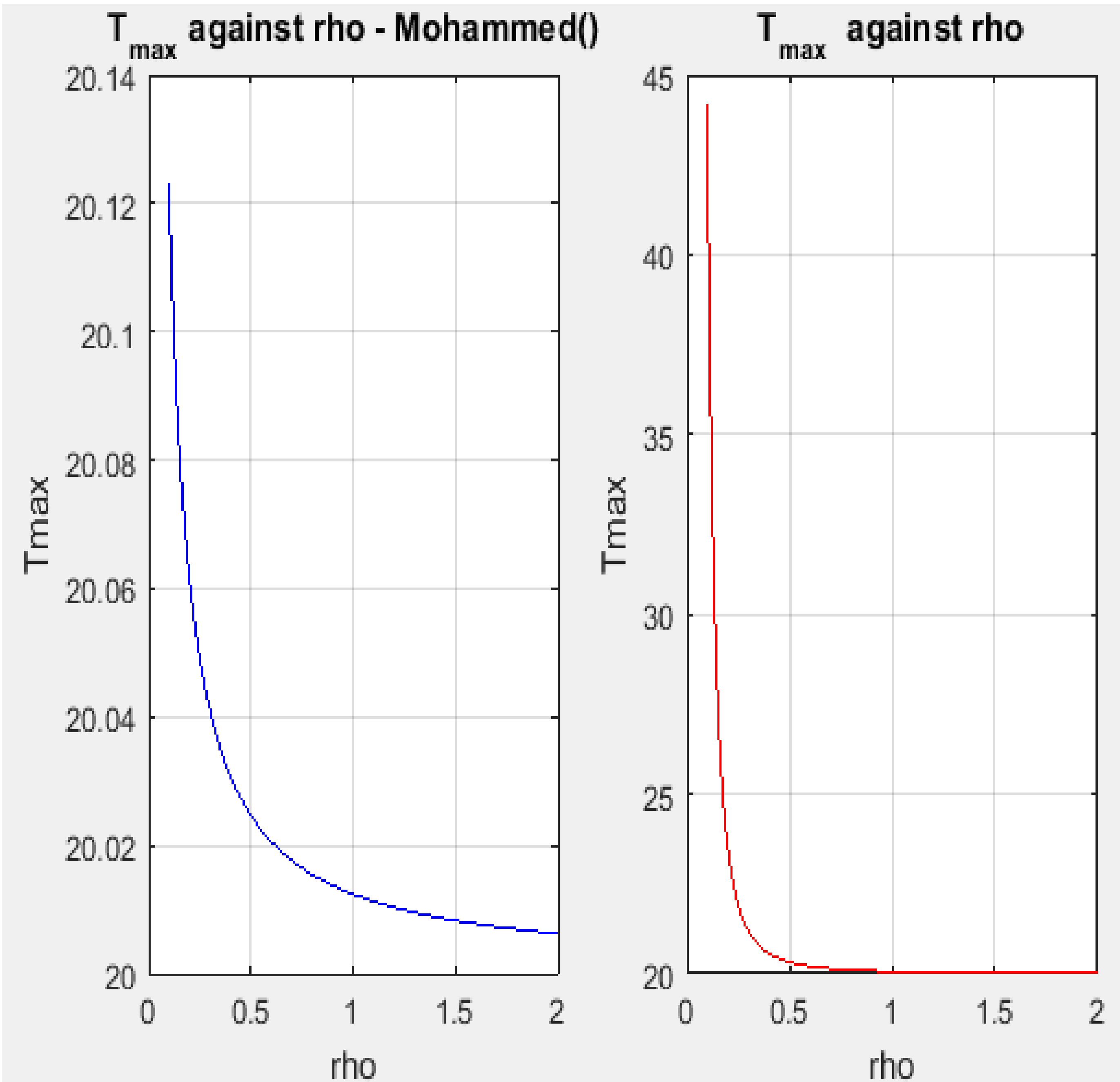

Figure 5.4: Variation of T_{max} with ρ at $T = 1.3$

Appendix-XVI

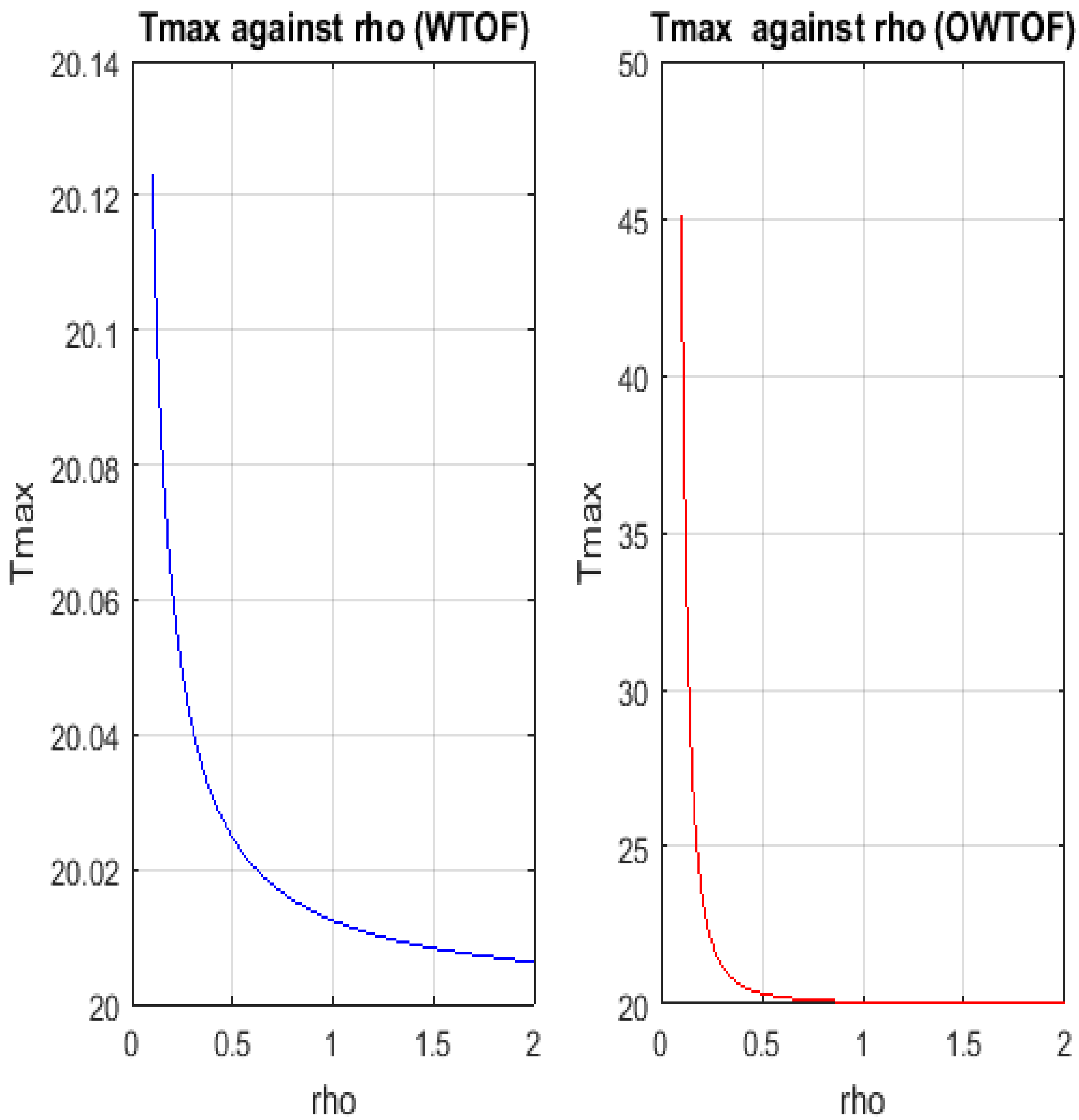

Figure 5.5: Variation of T_{max} with ρ at $T = 1.5$

Appendix-XVII

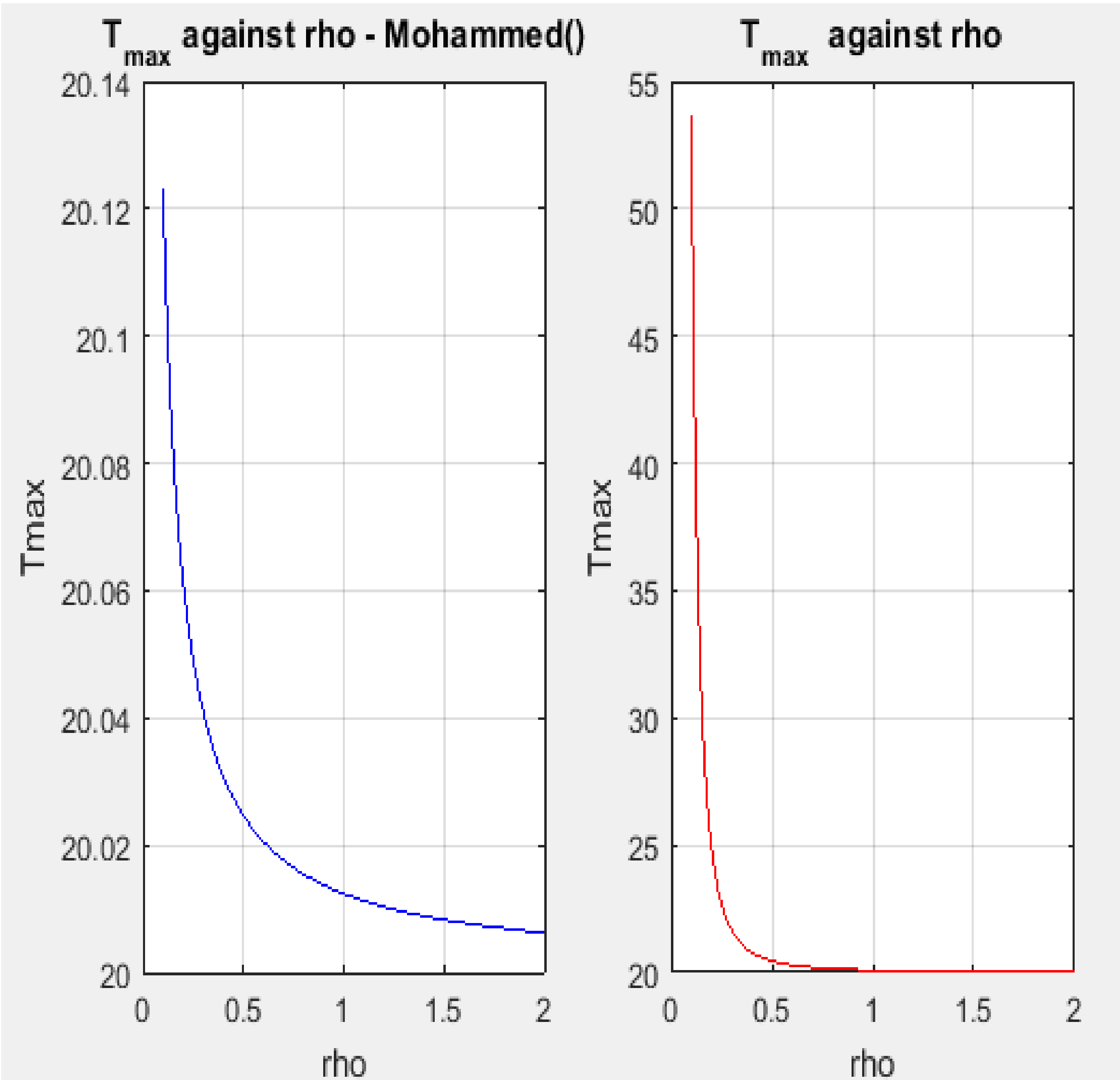

Figure 5.6: Variation of T_{max} with ρ at $T = 1.6$

Appendix-XVII

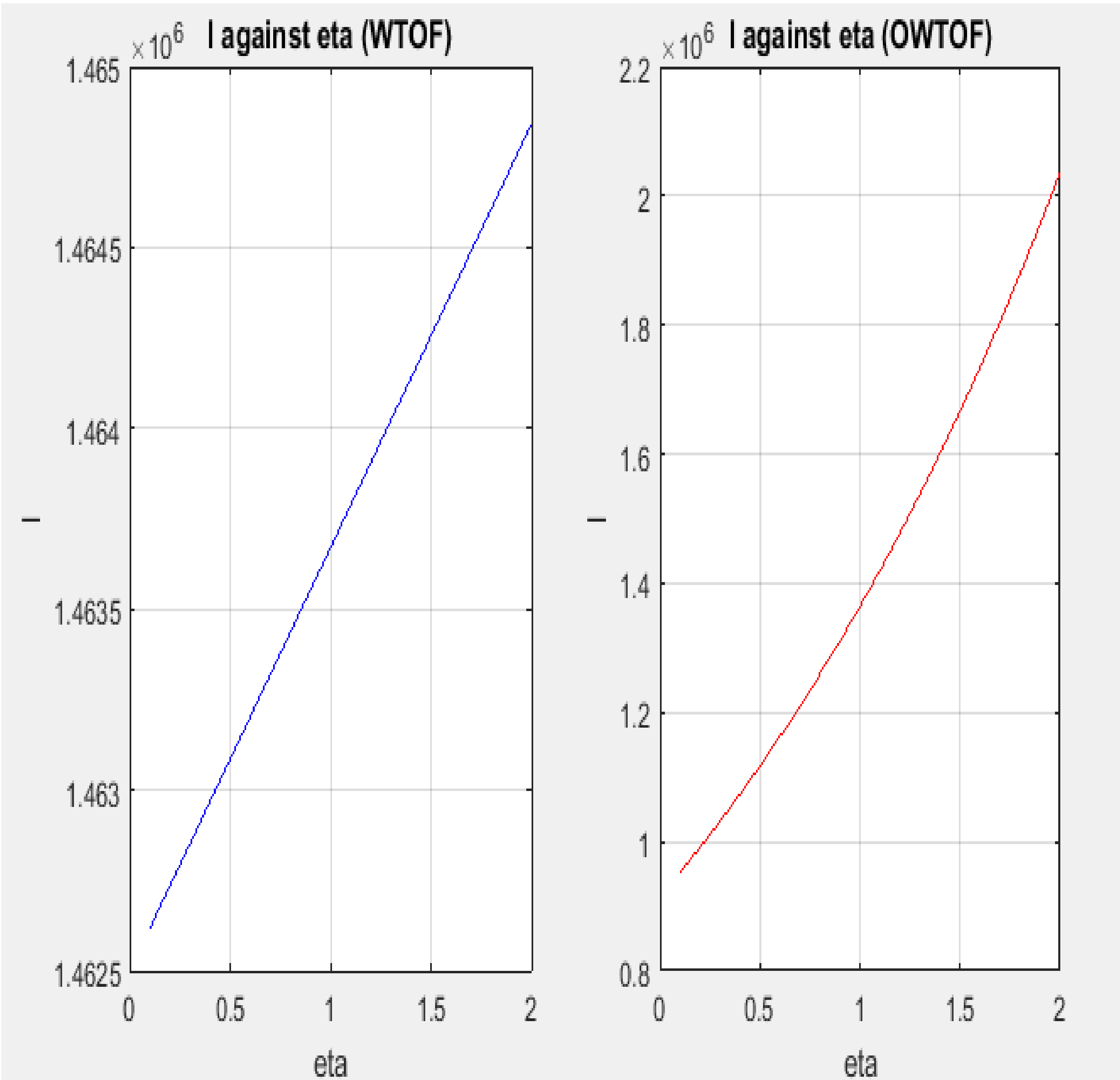

Figure 5.7: Variation of l with η at $T = 1.02$

Appendix-XIX

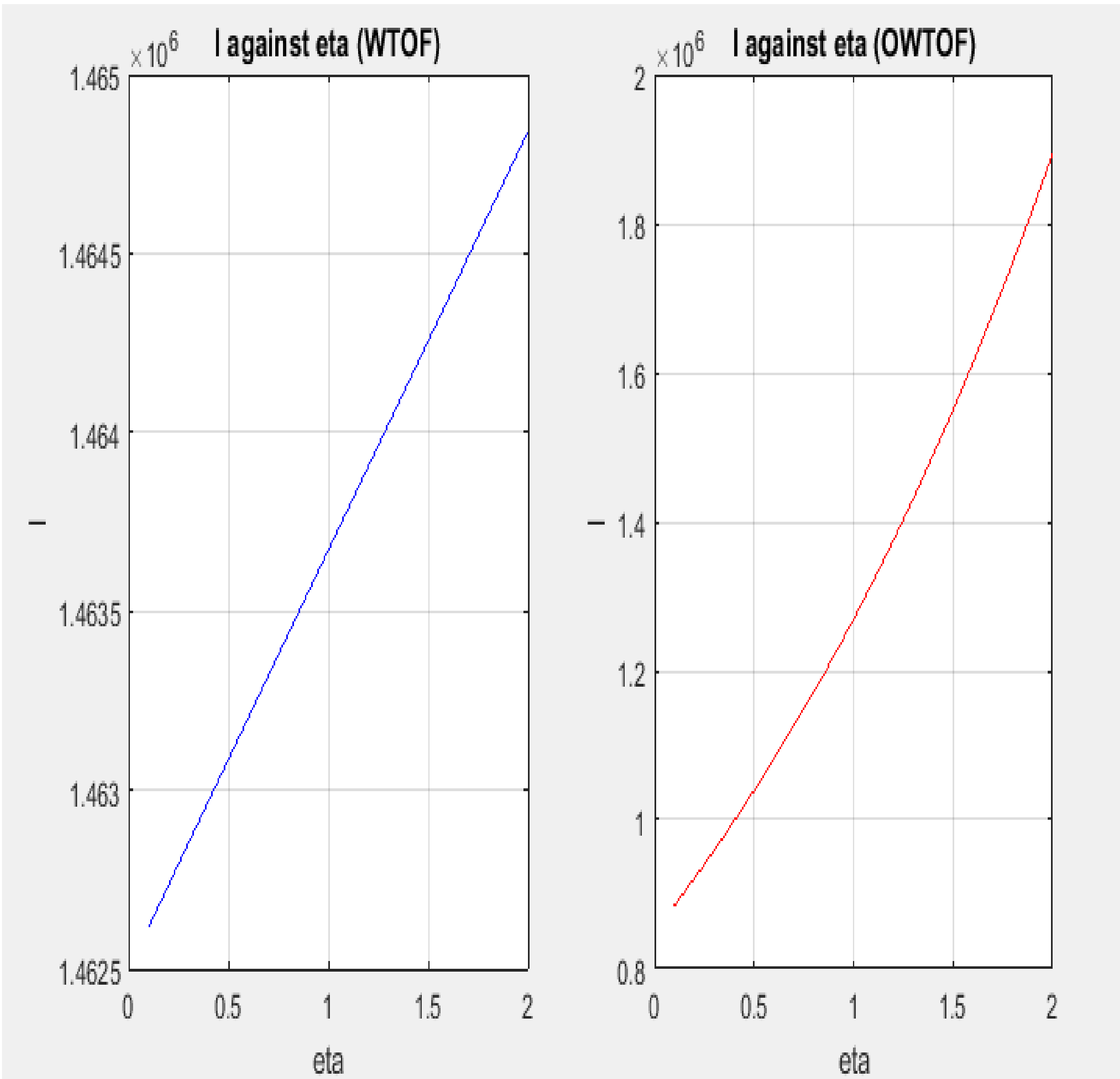

Figure 5.8: Variation of l with η at $T = 1.04$

Bibliography

[1] A. A. F. Junior, O. L. Coutinho, C. S. Martins and W. Santos. (2013). Effect of Fiber Optic Chromatic Dispersion on the Performance of Analog Optical Link with External Modulation Aiming at Aerospace Applications *J. Aerosp. Technol. Manag., So Jos dos Campos,* 5(2), 205-216, Jun. 2013.

[2] A. Chraplyvy. (2009). The coming capacity crunch *Plenary talk, European Conference on Optical Communications (ECOC),* Vienna, Austria.

[3] A. M. Rocha, P. S. Andre, M. Facao, P. Antunes and A. Martins. (2010). Evaluation of the fuse effect propagation in networks infrastructures with different types of fibers *Proceedings of Conference on Optical Fiber Communication, collocated National Fiber Optic Engineers Conference*, JWA10, San Diego, CA, USA.

[4] B. Yang, Y. Wang, Y. Liu, J. Sasian and J. Koshel. (2009). Efficient ray-tracing for free-form reflectors *Optik (Stuttg),* 120, 4044.

[5] C. Raack, M. Grtschel and A. Werner. (2014). Towards optimizing the deployment of optical access networks *EURO J Comput Optim,* 2, 1753.

[6] D. J. Richardson. (2013). Space-division multiplexing in optical fibers *Nat. Photon.* 7, 354.

[7] F. Wang, J. S. Jensen, and O. Sigmund. (2011). Robust topology optimization of photonic crystal waveguides with tailored dispersion properties *Opt. Soc. Am. B* 28(3).

[8] G. Bechtel. (2001). Optical IC market, WDM Solutions *Optical Sensor Technology* 21(3), 373-3745.

[9] G. D. Peng, P. L. Chu, L Xia and R. A. Chaplin. (1995). Fabrication and characterization of polymer optical fibers *",J. of IREEA,* 15(3), 289-296.

[10] H. Hemmati. (2006). Deep Space Optical Communication *John Wiley Sons, New York.*

[11] H. Kaushal, V. Kumar, A. Dutta, H. Aennam, H. Aennam, V. Jain, S. Kar, and J. Joseph. (2011). Experimental study on beam wander under varying atmospheric turbulence conditions *IEEE Photon. Tech. Lett.,* 23(22), 1691-1693.

[12] H. Thienpont, H. Murat, H. Smet, D. Cuypers, Y. Meuret, M. Vervaeke and L. Desmet. (2005). Increased lumens peretendue by combining pulsed LEDs *In Proc. SPIE,* 5740.

[13] I. Kask, V. Matjec, M. Chomt, D. Berkov and J. Probotov. (2004). silica-based optical fibers with refractive-index profiles tailored in a region of 1.45 - 1.62 for fiber-optic chemical detection. *Proc. 7th Europt(r)ode , Sensors Actuators, v tisku,* 27.

[14] I. S. Mohamed, H. A. Moustafa and M. B. Saleh. (2009). Axial Temperature Distribution in W-Tailored Optical Fibers *https://www.researchgate.net/publication/275300640.*

[15] J. M. Manceau, A. Averchi, F. Bonaretti, D. Faccio, P. Di Trapani, A. Couairon and S. Tzortzakis. (2009). Terahertz pulse emission optimization from tailored femtosecond laser pulse filamentation in air *optics letters* 34(14).

[16] J. Wiener. (2007) Measurement: Reliability and Validation Measures John Hopkins University, 1-27.

[17] K. S. Friis and Sigmund. (2012). Topology optimization of optical surfaces *10th International Symposium on Photonic and Electromagnetic Crystal Structures, Santa Fe, NM,* United states.

[18] M. J. Hamp, J. Wrigtht, M. Hubbard and B. Brimacombe. (2002). Investigation into the temperature Dependence of Chromatic Dispersion in Optical Fiber *IEEE Photon. Technol. Lett,* 14, 1524-1526, Nov. 2002.

[19] M. S. A. Rahman and B. C. Ng. (2008). MATLAB-based graphical user interface development for Centralized Failure Detection System (CFDS) in SCAN Network *J. of Opt. Commun.,* 29(3), 152-156.

[20] O. Cohen, J. S. Lundeen, B. J. Smith, G. Puentes, P. J. Mosley, and I. A. Walmsley. (2009). Tailored Photon-Pair Generation in Optical Fibers. *PhysRevLett.*102,123-603.

[21] P. Andre, A. Rocha, F. Domingues and M. Faco. (2011). Thermal Effects in Optical Fibers. *www.intechopen.com* Instituto de Telecomunicaes and Departamento de Fsica, Universidade de Aveiro Portugal .

[22] P. G. Kokaje, R. S. Kawitkar and M. S. Balan. (2015). Review of Recent Development in Optical Fiber Technology *Internation Journal of Advanced Research in Electrical, Electronics and Instrumentation Engineering,* 4(3).

[23] P. S. Andr, A. N. Pinto, J. L. Pinto. (2004). Effect of Temperature on the Single Mode Fiber Chromatic Dispersion *Journal of Microwaves and Optoelectronics,* 3(5), July 2004.

[24] R. G. Smith. (1972). Optical power handling capacity of low loss optical fibers as determined by stimulated Raman and Brillouin scattering *Applied Optics,* 11, 2489-2494.

[25] R. J. Essiambre and R. W. Tkach. (2012). Capacity trends and limits of optical communication networks *Proc. IEEE,* 100(5), 10-35.

[26] R. Romaniuk and J. Dorosz. (1998). Multi-crucible technology of tailored optical fibers *Optica Applicata.* 28(4), 293-322.

[27] R. S. Romaniuk and W. Wjcik. (2010). Development of optical fiber technology in poland *Int journal of electronics and telecommunications,* 56(1), 990104.

[28] R. W. Tkach. (2010). Scaling optical communications for the next decade and beyond *Bell Labs Tech. J,* 14, 3.

[29] S. K. Tripathy, G. M. Carter, Y. J. Chen, M. F. Rubner, D. J. Sandman, M. K. Thakur and in D. Chemla and J. Zyss (eds.). (1986). Nonlinear Optical Phenomena in Organic and Polymeric Solids *Acac ,mic Press, in press, Synthetic Metals,* 15, 229-235.

[30] S. Kumar and Y. C. Bhatt. (2014). fiber cable fault management system *international journal of advance research in science and engineering,* 3(2), February 2014.

[31] S. P. Singh and N. Singh. (2007). nonlinear effects in optical fibers: origin, management and applications *Progress In Electromagnetics Research, PIER,* 73, 249-275.

[32] S. Ramamurthy, B. Mukherjee, and L. Sahasrabuddhe. (2003). Survivable WDM mesh networks *Journal of Lightwave Technology,* 21(4), 870-883.

[33] S. Ramamurthy and B. Mukherjee. (2004). review of fault management in WDM mesh networks: basic concepts and research challenges *IEEE Network,* 18(2).

[34] T. D. Engeness, M. Ibanescu, S. G. Johnson, O. Weisberg, M. Skorobogatiy, S. Jacobs, and Y. Fink. (2003). Dispersion tailoring and compensation by modal interactions in OmniGuide *Fiber optics and optical communications.*

[35] T. G. Giallorenzi, G. H. Sigel, J. H. Cole, S. C. Rashleigh and R. G. Priest. (1982). special on Optical fiber sensor technology *https//www.link.spring.com, IEEE JQE,* 18(4), 626-665.

[36] T. Morioka. (2009). New generation optical infrastructure technologies: EXAT initiative towards 2020 and beyond *Proc. Optoelectron. Commun. Conf. (OECC).*

[37] T. Okoshi and K. Oyamoda. (1982). Side tunnel fibre: an approach to polarization maintaining optical wave guiding scheme *Electronics Letters,* 18, 824-826.

[38] T. Shimura. (1990). Decomposition of non-decreasing slowly varying function and the domain of attraction of Gaussian distributions *J.Math. Soc. Japan*, 43(4), 1-19.

[39] W. Nowacki and I. N. Sneddon. (1974). Thermodynamics in Solids, Springer Verlag *Proc. IEEE.*

[40] Z. Ghassemlooy and W. O. Popoola. (2010). Terrestial Free-Space Optical Communications *InTech,* ch.17, 356392.

[41] Z. H. Jiang, S. Yun, L. Lin, J. A. Bossard, D. H. Werner and T. S. Mayer. (2012). Tailoring Dispersion for Broadband Low-loss Optical Metamaterials Using Deep-sub wavelength Inclusions *www.nature.com/scientificreport,* 3, 1571.